Production of Calcium–Mobilizing Metabolites by a Novel Member of the ADP–Ribosyl Cyclase Family Expressed in Schistosoma mansoni

DATASET · SEPTEMBER 2005

13 AUTHORS, INCLUDING:

Production of Calcium-Mobilizing Metabolites by a Novel Member of the ADP-Ribosyl Cyclase Family Expressed in *Schistosoma mansoni*[†,‡]

Stephen P. Goodrich,[§] Hélène Muller-Steffner,[||] Ahmed Osman,[⊥] Marie-Jo Moutin,[#] Kim Kusser,[§] Alan Roberts,[§] David L. Woodland,[§] Troy D. Randall,[§] Esther Kellenberger,[▽] Philip T. LoVerde,[⊥] Francis Schuber,[||] and Frances E. Lund*,[§]

Trudeau Institute, 154 Algonquin Avenue, Saranac Lake, New York 12983, Laboratoire de Chimie Bioorganique, UMR 7514 CNRS/ULP, and Bioinformatics of the Drug, UMR 7081 CNRS/ULP, Faculté de Pharmacie, 74 route du Rhin 67400 Strasbourg-Illkirch, France, Department of Microbiology and Immunology, School of Medicine and Biomedical Sciences, State University of New York, 3435 Main Street, Buffalo, New York 14214, and Laboratoire Canaux Calciques Fonctions et Pathologies, INSERM U-607, 17 rue des Martyrs, 38054 Grenoble, Cèdex 9, France

ABSTRACT: ADP-ribosyl cyclases are structurally conserved enzymes that are best known for catalyzing the production of the calcium-mobilizing metabolite, cyclic adenosine diphosphate ribose (cADPR), from nicotinamide adenine dinucleotide (NAD^+). However, these enzymes also produce adenosine diphosphate ribose (ADPR) and nicotinic acid adenine dinucleotide phosphate ($NAADP^+$), both of which have been shown to modulate calcium mobilization in vitro. We have now characterized a new member of the cyclase family from *Schistosoma mansoni*, a member of the Platyhelminthes phylum. We show that the novel $NAD(P)^+$ catabolizing enzyme (NACE) expressed by schistosomes is structurally most closely related to the cyclases cloned from *Aplysia* but also shows significant homology with the mammalian cyclases, CD38 and CD157. NACE expression is developmentally regulated in schistosomes, and the GPI-anchored protein is localized to the outer tegument of the adult schistosome. Importantly, NACE, like all members of the cyclase family, is a multifunctional enzyme and catalyzes NAD^+ glycohydrolase and base-exchange reactions to produce ADPR and $NAADP^+$. However, despite being competent to generate a cyclic product from NGD^+, a nonphysiologic surrogate substrate, NACE is so far the only enzyme in the cyclase family that is unable to produce significant amounts of cADPR (<0.02% of reaction products) using NAD^+ as the substrate. This suggests that the other calcium-mobilizing metabolites produced by NACE may be more important for calcium signaling in schistosomes. Alternatively, the function of NACE may be to catabolize extracellular NAD^+ to prevent its use by host enzymes that utilize this source of NAD^+ to facilitate immune responses.

Cyclic adenosine diphosphate ribose (cADPR)[1] was described more than 15 years ago as a calcium (Ca^{2+})-mobilizing metabolite present in extracts isolated from the gastropod *Aplysia californica* (*1*). The enzyme(s) that catalyze the transformation of nicotinamide adenine dinucleotide (NAD^+) into cADPR (ADP-ribosyl cyclases) were first purified and cloned from two different *Aplysia* species (*2−5*). Based on the five invariant intradisulfide bond structure of these two proteins they were classified in a new enzyme family (*6*). Subsequently, several other proteins with homology to the *Aplysia* cyclases were identified and added to the cyclase family of enzymes including two plasma membrane-associated mammalian proteins, CD38 (*7, 8*) and CD157 (BST-1) (*9−11*). Importantly, the 10 cysteine residues that form the invariant intradisulfide bonds in the *Aplysia* cyclase were conserved in CD38 and CD157. Likewise, the key catalytic and substrate binding residues that had been identified in the *Aplysia* cyclases (*12, 13*) were also conserved in CD38 and CD157 (*6*). The three-dimensional structures of the *A. californica* cyclase (*6*) and the ecto-domain of CD157 (*14*) were found to be strikingly similar, particularly within the highly conserved active site region referred to as the "TLED signature domain" (*15*). Finally, as expected, both CD38 (*16−19*) and CD157 (*20*) were able to catalyze the ADP-ribosyl cyclase reaction and produce cADPR, although in much lower yields than the *Aplysia* cyclases.

Cyclic ADP-ribose is only one of three Ca^{2+}-mobilizing metabolites produced by cyclases. In fact, the cyclases are

---

[‡] The nucleotide sequence for NACE was deposited in GenBank accession number AY826981.

* Author to whom correspondence should be addressed. Tel: 518-891-3080. Fax: 518-891-5126. E-mail: flund@trudeauinstitute.org.

[§] Trudeau Institute.

[||] Laboratoire de Chimie Bioorganique, UMR 7514 CNRS/ULP.

[⊥] State University of New York.

[#] Laboratoire Canaux Calciques Fonctions et Pathologies, INSERM U-607.

[▽] Bioinformatics of the Drug, UMR 7081 CNRS/ULP.

[1] Abbreviations: ryanodine receptor, RyR; inositol trisphosphate, IP3; cyclic adenosine diphosphate ribose, cADPR; adenosine diphosphate ribose, ADPR; nicotinamide adenine dinucleotide, NAD^+; nicotinic acid adenine dinucleotide, $NAADP^+$; relative fluorescence unit, RFU; 1,N^6-etheno-NAD^+, ϵ-NAD^+; phosphatidylinositol phospholipase C, PI-PLC; nicotinamide guanine dinucleotide, NGD^+.

multifunctional enzymes that are not only able to cyclize NAD^+ to produce cADPR (ADP-ribosyl cyclase reaction) but also able to hydrolyze NAD^+ (NAD^+ glycohydrolase reaction) to produce adenosine diphosphate ribose (ADPR) (*16*) and to perform a base-exchange (transglycosidation reaction) with $NADP^+$ to produce nicotinic acid adenine dinucleotide phosphate ($NAADP^+$) (*21, 22*). Both cyclic ADP-ribose and ADPR have been shown to mediate intracellular Ca^{2+} release by an inositol trisphosphate (IP_3)-independent (*23*), ryanodine receptor (RyR)-dependent mechanism (*24−31*). In contrast, ADPR activates Ca^{2+} influx in mammalian cells by activating the plasma membrane ion channel, TRPM2 (*32−34*). Thus, cyclases have the ability to produce second messengers that mobilize multiple independent sources of calcium.

Given the unique ability of cyclases to produce multiple Ca^{2+}-mobilizing metabolites, it was predicted that cyclases likely play physiologically important roles in Ca^{2+} signaling. In agreement with this hypothesis, cADPR was shown to regulate numerous cell processes including contraction, secretion, exocytosis, and fertilization (*35*). Likewise, using gene-targeted CD38 deficient mice (*36, 37*) we and others showed that CD38 regulates immune responses (*38, 39*), smooth muscle contractility (*40, 41*), glucose tolerance (*37*), and osteoclast function (*42*). Importantly, the defects observed in the CD38 deficient mice appear to be due, at least in part, to the loss of cADPR, resulting in aberrant Ca^{2+} mediated signaling (*37−41, 43, 44*).

Since CD38 and cADPR clearly regulate signal transduction and modulate important biologic processes in mice, we set out to identify and characterize novel cyclases from other organisms. In this manuscript, we report the cloning and biochemical characterization of a new member of the cyclase family isolated from the Platyhelminth, *Schistosoma mansoni*. *S. mansoni* is one of the etiologic agents of schistosomiasis, a disease that ranks in importance with malaria and tuberculosis as it afflicts some 300 million people in 76 countries (*45*). We demonstrate that the *Schistosoma* enzyme (referred to as $NAD(P)^+$ catabolizing enzyme or NACE) is structurally very similar to all of the other cyclase family members, is developmentally regulated in schistosomes, and is expressed as a GPI-anchored protein on the outer tegument of adult worms. NACE is able to catalyze $NAD(P)^+$ glycohydrolase and base-exchange reactions to produce ADPR and $NAADP^+$. However, in striking contrast with all of the other members of the ADP-ribosyl cyclase family, NACE is unable to produce significant quantities of the signature metabolite cADPR from NAD^+, despite being competent to catalyze a cyclase reaction with the surrogate substrate NGD^+. Thus, since NACE is biochemically distinct from other members of the cyclase family, it is likely to perform novel functions in schistosomes.

MATERIALS AND METHODS

NACE Cloning. A blast search using the consensus amino acid sequence for cyclase family members (*6*) was performed, and an EST isolated from *S. mansoni* (Accession No. AW017229) was identified. Primers specific for the EST (see Supporting Information Figure S1A) were synthesized (Sigma/Genosys), and the 330 bp cDNA was cloned by PCR amplification from a Lambda ZAP II cDNA library con-

structed from polyA$^+$ mRNA isolated from adult worm pairs (*46*). The sequence of the cDNA clone was verified, and the PCR product was used as a probe to isolate a full length clone containing the entire coding sequence (NACE-native; Accession No. AY826981). The nucleotide and amino acid sequence for the *S. mansoni* NACE was used in a BLAST search to identify the *Schistosoma japonicum* NACE orthologue (Accession No. AY222890) (*47*).

NACE Sequence Comparisons and Structural Modeling. The amino acid sequence of *S. mansoni* NACE was aligned with the reported sequences for members of the cyclase family using the CLUSTAL W multiple sequence alignment program (http://www.ebi.ac.uk/clustalw/) (*48*). The phylogram analysis comparing the relatedness of *S. mansoni* NACE with all other known cyclase family members was performed with an evolutionary relationship program (http://www.ebi.ac.uk/clustalw/). The three-dimensional structure of NACE was obtained by homology modeling based on the crystallographic coordinates of both *Aplysia* ADP-ribosyl cyclase (PDB entry 1lbe) and human BST1/CD157 (PDB entry 1isf) using Modeller (*49*) and energy minimization using AMBER 5.0.

NACE Constructs. The primary nucleotide sequence of *S. mansoni* NACE (NACE-native) was optimized for mammalian codon usage, resynthesized (GENEART, Regensburg, Germany), and then cloned into the mammalian expression vector pcDNA3.1 (referred to as NACE-opt). To facilitate immunoprecipitation and immunofluorescence analysis of NACE-opt, the 5′ leader sequence of NACE-native (see Supporting Information Figure S2 for sequence), identified by the SignalP (http://www.cbs.dtu.dk/services/SignalP/) (*50*) and Phobius programs (http://phobius.binf.ku.dk/) (*51*), was replaced with the mammalian CD8α leader sequence and a FLAG tag (ref *16*; construct referred to as CD8L/FLAG-NACE). To produce recombinant soluble NACE in COS-7 cells, the GPI-anchor sequence, identified by the consensus sequence for the ω site (site of GPI attachment, see Figure S2 for sequence (*52*)), was removed from CD8L/FLAG-NACE (construct referred to as CD8L/FLAG-NACEΔGPI). To produce soluble recombinant NACE in yeast, the 5′ leader sequence and the 3′ GPI-anchor sequences were eliminated from NACE-opt and the remaining core ecto-domain sequence was cloned into the *Pichia pastoris* expression vector pPICZα A (Invitrogen, construct referred to as solNACE-Y). All constructs were sequenced to ensure that the insertions and truncations were present and that no artifacts had been introduced to the rest of the NACE coding region during the cloning process.

Generation and Purification of Polyclonal Antiserum to NACE. C57BL/6J mice were bred and maintained in the Trudeau Institute Animal Breeding facility. All procedures involving animals were approved by the Trudeau Institute Institutional Animal Care and Use Committee and were conducted according to the principles outlined by the National Research Council. Mice were vaccinated on days 0, 28, and 56 using a Helios Gene Gun (Bio Rad) with 2.1 μm diameter gold bullets that were coated with the CD8L/FLAG-NACE vector (1 μg/bullet) and the adjuvant vector, pBOOST-mIL-4/IL1β (0.25 μg/bullet, Invivogen). Serum was collected from vaccinated mice between days 10 and 70 and was pooled, and the IgG-containing fraction was

enriched using a Melon Gel IgG Spin Purification kit (Pierce).

NACE Expression. To express NACE in mammalian cells, COS-7 cells were transiently transfected with the various NACE constructs described above using Lipofectamine 2000 (Gibco). At 72 h the conditioned media and/or cells were harvested from the plates and analyzed. To express recombinant soluble NACE in yeast, *P. pastoris* strain GS115 (Invitrogen) was electroporated with the solNACE-Y construct and plated in medium containing zeocin. Transformants were grown according to a previously described protocol (*53*) and induced with methanol for 48 h at 30 °C. A high-expressing clone was selected and used for large-scale production.

Purification of Soluble Recombinant NACE. To purify soluble recombinant NACE from transfected COS-7 cells, the conditioned medium was collected 72 h post-transfection, adjusted to a final concentration of 150 mM NaCl, filtered, and then passed over an ANTI-FLAG M2-agarose affinity gel column (Sigma). The FLAG-tagged NACE was eluted with 200 μg/mL FLAG Peptide (Sigma), and the protein concentration from the pooled and concentrated fractions was determined with the Nano Drop ND-1000 spectrophotometer (Nano Drop Technologies, Wilmington DE) using BSA as a standard.

Recombinant NACE, secreted as a soluble protein in the supernatant of methanol-induced *P. pastoris*, was purified in a single step on a 1.2 × 4-cm Blue Sepharose 6 fast flow CL-6B column (Amersham Biosciences). After dialysis against 10 mM potassium phosphate buffer (pH 7.4), the medium was loaded at 2 mL/min and the enzyme was eluted with a linear 0−1.5 M gradient of NaCl in the same buffer. The protein concentration was determined by the BCA protein assay (Pierce) using BSA as a standard.

Silver Stain and Western Blot Analysis. Proteins were separated by electrophoresis and were either transferred to PVDF-Plus (Osmonics) for Western blot analysis or were fixed, washed, and stained with GelCode SilverSNAP silver stain kit (Pierce). Western blot membranes were stained with biotinylated anti-FLAG (Sigma, 0.5 μg/mL) or anti-NACE antiserum (1:2000 dilution) at 4 °C for 1.5 h, washed, and then incubated with either streptavidin-HRP (Southern Biotechnology) or anti-mouse Ig-HRP (Jackson Immunoresearch) for 1.5 h. Blots were developed using either fast- or slow-developing chemiluminescence kits (Amersham).

Immunofluorescence Analysis. COS-7 cells were transiently transfected in Lab Tek slide chambers (Nunc) with NACE constructs or an empty vector control. At 72 h post-transfection, the cells were fixed with 4% paraformaldehyde for 5 min and then washed and blocked in dPBS containing 5% BSA. To detect NACE using the mouse anti-NACE antiserum, slides were stained with anti-NACE (1:750 dilution) or normal mouse serum (1:750), washed, and then stained with donkey anti-mouse IgG-Alexa-594 (Molecular Probes). To detect the FLAG tag of CD8L/FLAG-NACE, slides were incubated with avidin/biotin block (Vector), probed with biotinylated mouse anti-FLAG antibody (Sigma), washed, and then developed with streptavidin Alexa Fluor 594 (Molecular Probes). All slides were counterstained with DAPI mount (Molecular Probes) and viewed with a Zeiss Axioplan 2 microscope (Oberkochen, Germany) under bright field and fluorescence using the appropriate band-pass filters.

Images were captured using a 40× objective with a Zeiss AxioCam digital camera and were overlayed using the Zeiss proprietary software, Axiovision 3.0.6.0.

Localization of NACE in S. mansoni Parasites. Cryosections of adult worms were probed with affinity-purified IgGs isolated from anti-NACE mouse serum (5 μg/mL) or purified normal mouse IgG. After washing, the sections were then stained with biotinylated secondary anti-mouse IgG (5 μg/mL; Jackson Immunoresearch), washed, and then stained with the far-red fluorophore, Alexa Fluor 647-conjugated streptavidin (5 μg/mL; Molecular Probes). Live and acetone-fixed parasites (adult worms and mechanically transformed schistosomules; 3 h old) were whole-mounted and stained with anti-NACE IgG as described for the cryosections. Cryosections and whole mount parasites were examined using a Bio-Rad MRC-1024 confocal microscope equipped with krypton−argon laser and 522 and 650 nm filters. NACE was visualized with Alexa Fluor 647 which emits at a maximum wavelength of 668 nm, where autofluorescence produced by phenolic compounds in schistosome sections is not detected. The fluorescent three-dimensional structures of whole mount adult worms were reassembled from the submicron laser sections using a voxel-based three-dimensional (3-D) imaging program (Voxx, v. 2 (*54*)).

Fluorometric Enzyme Assays. NAD$^+$ glycohydrolase activity was assayed fluorometrically using 1,N^6-etheno-NAD$^+$ (ϵ-NAD$^+$, Sigma) as previously described (*55*). Briefly, aliquots of cell lysates, conditioned media, purified NACE protein (25−200 ng), NACE immunoprecipitated on Sepharose beads (25 μL beads) or live *S. mansoni* worms (10 worms/assay) were incubated in the presence of 40−400 μM ϵ-NAD$^+$ (100 μL final volume) at 37 °C in a SpectraMAX GeminiXS fluorescence plate reader (Molecular Devices, Sunnyvale, CA). The fluorescence emission at 410 nm (excitation at 300 nm) of the fluorescent product ϵ-ADPR was then followed for the next 30 min. Data is represented in relative fluorescence units (RFU) after blanking at time 0. The GDP-ribosyl cyclase activity was assayed similarly using NGD$^+$ (Sigma, 80−800 μM) as the substrate (*56*) and following the appearance of the fluorescent product cyclic GDP-ribose (emission 410 nm, excitation 310 nm).

ADP-ribosyl cyclase activity was determined using a cycling assay to detect cADPR (*57*). Purified recombinant NACE was incubated with NAD$^+$ (200 μM) in 10 mM potassium phosphate buffer (pH 7.4) (1 mL final volume) until the reaction reached 50% completion. The enzyme was eliminated by centrifugation for 10 min at 5000g on ultrafiltration units (Vivaspin 2,Vivascience). The contaminating nucleotides were removed, and the sample was then incubated 1 h at room temperature with 0.1 μg/mL *A. californica* ADP-ribosyl cyclase and 10 mM nicotinamide in 100 mM sodium phosphate buffer, pH 8.0. The cycling reaction was then allowed to proceed in the same buffer in the presence of 0.8% ethanol, 10 mM nicotinamide, 40 μg/mL BSA, 20 μg/mL diaphorase (treated with charcoal), 20 μg/mL alcohol dehydrogenase, 10 μM FMN, and 20 μM resazurin. The increase in resorufin fluorescence (excitation at 544 nm and emission at 590 nm) was measured every minute for 2 h using a fluorescence plate reader (FluoStar from BMG Labtechnologies Inc).

Nonfluorometric Enzyme Assays. All three activities of NACE were measured using recombinant enzyme purified

from *P. pastoris*. The NAD^+ glycohydrolase activity was measured under saturating (420 μM) or limiting (25 μM) amounts of NAD^+ in the presence of [adenosine-U-^{14}C]-NAD^+ (2.5 × 10^5 dpm) as previously described (*58*). Briefly, the enzyme was incubated at 37 °C with substrate and, at selected times, aliquots were removed and treated with ice-cold perchloric acid to stop the reaction. After neutralization, the precipitated proteins were removed by centrifugation and product formation was then monitored by HPLC. The same experimental conditions were used with NGD^+ to assay both NGD^+ glycohydrolase and GDP-ribosyl cyclase activities.

The cADPR hydrolase activity was measured by incubating cADPR (20 μM) at 37 °C in 10 mM potassium phosphate buffer (pH 7.4) in the presence of enzyme. Aliquots were removed at different time points, treated as described above, and analyzed by HPLC on a C_{18} column.

The transglycosidation of $NADP^+$ was measured by incubating recombinant soluble NACE with 1 mM $NADP^+$ and 20 to 40 mM nicotinic acid at 37 °C for 20 min in a 10 mM potassium phosphate buffer, pH 6.0 or 7.4. The reaction mixture was analyzed by HPLC on an ion-exchange column (see below).

Analysis of Reaction Products by HPLC. The formation of $NAADP^+$ was assessed by analysis on a 150 × 4.6 mm AG MP-1 column (Interchrom) using a Shimadzu HPLC system. The elution was performed at a flow rate of 1 mL/min with a nonlinear gradient starting with 100% solvent A (water). The percentage of solvent B (1.5% TFA) was linearly increased to 1% in 2 min, 2% in 4 min, 4% in 9 min, 8% in 13 min, 16% in 17 min, 32% in 21 min, 100% in 25 min and maintained at 100% for 10 min. Peaks were identified by comparison with authentic samples, and areas obtained from UV recordings were normalized using the molar extinction coefficients of the reaction products. Analysis of all other products was performed by HPLC on a 300 × 3.9 mm μBondapak C_{18} column (Waters Assoc.) as previously described (*58*). The eluted compounds were detected by radiodetection (Flo-one, Packard Radiometric Instruments, Meriden CT) when using [^{14}C]NAD^+ or by absorbance recordings at 260 nm when using NGD^+ or unlabeled NAD^+.

Enzyme Kinetics. The assays were conducted at 37 °C in the presence of soluble recombinant enzyme using eight different substrate concentrations. Reaction progress was obtained either by HPLC analysis of aliquots removed at given times or, alternatively, in the case of NGD^+, by monitoring the change of fluorescence at 410 nm (λ_{exc} = 310 nm). Kinetic parameters were determined from the plots of the initial rates as a function of substrate concentration, according to Michaelis−Menten kinetics, using a nonlinear regression program (GraphPad, Prism).

Preparation of Cell and Worm Lysates and Membrane Microsomes. COS-7 cells were transiently transfected with NACE expression constructs or empty vector for 72 h. Cells were collected, washed in dPBS, and frozen. Adult *S. mansoni* worm pairs were collected from the portal vein of 45 day infected golden hamsters, washed in dPBS, and frozen. COS-7 cell pellets and worm pellets were lysed in 10 mM Tris/HCl (pH 7.3), 0.4 mM EDTA, protease inhibitors, and 1% Triton X-100 (v/v), and detergent-soluble proteins were collected. In some experiments, the total lysates were used to analyze NACE enzyme activity, while in other

experiments, NACE was immunoprecipitated from the lysates using either Anti-FLAG Sepharose beads or protein G beads coated with anti-NACE antiserum.

To prepare membrane fractions from adult *S. mansoni* worms, 2 g of worms were disrupted at 4 °C with a potter in 10 mM potassium phosphate buffer (pH 7.4) containing 1 mM EDTA and 0.1 mM phenylmethylsulfonyl fluoride (PMSF) as protease inhibitors. The homogenate was centrifuged at 10000g for 15 min and the postmitochondrial supernatant was centrifuged at 100000g for 60 min to obtain membrane microsomes. The membrane fraction was resuspended in 10 mM potassium phosphate buffer (pH 7.4).

Phospholipase C Treatment. To cleave GPI-anchored proteins from transiently transfected COS-7 cells, the cells were washed with HBSS at 48 h post-transfection and then resuspended in HBSS in the presence or absence of 0.2 unit of phosphatidylinositol-specific phospholipase C (PI-PLC from *Bacillus cereus*, Sigma) at 37 °C for 2 h. The medium was removed and assayed for NAD^+ glycohydrolase activity using ϵ-NAD^+ as a substrate. To cleave GPI-anchored proteins from *S. mansoni* membrane microsome fractions, 200 μL of the microsome prep was incubated in the presence or absence of 1 unit of PI-PLC for 2 h at 30 °C. The fractions were then centrifuged at 100000g for 60 min, and the supernatant and microsomes were tested for NAD^+ glyco-hydrolase and NGD^+ cyclase activity as described above. To cleave GPI-anchored proteins from *S. mansoni* adult worms, 10 live worms were suspended in 200 μL of HBSS in the presence or absence of 0.4 unit of PI-PLC at 37 °C for 2 h. The medium was collected and assayed for NAD^+ glycohydrolase activity, GDP-ribosyl cyclase activity, and pyrophosphatase activity as described above. Alternatively, the medium was electrophoresed on an SDS−PAGE gel and analyzed by silver staining or Western blot with the anti-NACE antibody as described above.

Endoglycosidase Treatment. CD8L/FLAG-NACE (70 ng) was incubated in 50 mM NaH_2PO_4 (pH 5.5) in the presence or absence of 0.05 unit of Endoglycosidase F1 (Sigma) for 1.5 h. The treated and untreated protein samples were then analyzed by SDS−PAGE and silver staining.

NACE mRNA Transcription Analysis. Analysis of NACE mRNA levels in different developmental stages was performed by semiquantitative RT-PCR as previously described (*59*). Briefly, total RNA was extracted from different developmental stages, representing growth in both mammalian and molluscan hosts, using TRIzol reagent (Invitrogen). Complementary DNA (cDNA) was prepared from the RNA samples using random decamer primers and was then used as the template in PCR reactions using specific primers for NACE (forward primer corresponding to bp 536−562; reverse primer complementary sequence of bp 836−862 of the NACE cDNA, yielding 327 bp PCR product) and for *S. mansoni* α-tubulin gene (GenBank Accession No. M80214; bp 424−444 and the complementary sequence of bp 777−801 as forward and reverse primers, respectively, yielding 378 bp PCR product). PCR reactions were separated by electrophoresis, analyzed using gel-documentation system (GelDoc1000; Bio-Rad) and quantified using Quantity One software (version 4.2.3; Bio-Rad). Expression of the constitutively present α-tubulin gene was used to normalize NACE expression in the various samples. To ensure that the amplification products were analyzed in the exponential

phase and below saturation limits (PCR plateau), the number of PCR cycles was also varied. Twenty-four cycles were used for α-tubulin while 26 cycles were used to amplify NACE PCR products.

RESULTS

Platyhelminthes Express a Novel Member of the ADP-Ribosyl Cyclase Family. Since the mammalian cyclase, CD38, plays an important functional role in regulating Ca^{2+} signaling in a variety of cell types (*60*), we thought it was important to identify other members of the cyclase family. Therefore, we used the published consensus sequence for ADP-ribosyl cyclases (*6*) to search the public DNA and protein databases and identified a single 330 bp EST (Accession No. AW017229) that was 27% similar at the amino acid level to the consensus cyclase sequence. Interestingly, the EST we identified was isolated from *S. mansoni*, a member of the phylum Platyhelminthes. To obtain the complete cDNA we designed PCR primers within the EST and used these primers to amplify the sequence from a *S. mansoni* cDNA library. We then used the PCR fragment to probe the *S. mansoni* cDNA library and identified a full-length clone of 1034 bp containing a 303 amino acid open reading frame that could give rise to a protein with a predicted molecular weight of 36 kDa (Figure S1A). The open reading frame for the novel *S. mansoni* gene encoded a protein that is 21% identical to the human cyclases CD38 and CD157 (37% and 38% similarity, respectively), and 24% identical to the *A. californica* cyclase (39% similarity, see Supporting Information Figure S1B). Importantly, the critical cysteine residues necessary for the 5 conserved intra-disulfide bonds found in most cyclases (*6*) are present in the novel *S. mansoni* sequence (Figure S1B). Likewise, the crucial catalytic glutamate (E202) found deep within the nicotinamide binding pocket of all known cyclases (*12*) and a substrate-binding tryptophan residue (W165) that lines the rim of the nicotinamide-binding pocket of cyclases (*12*) are both conserved in the novel *S. mansoni* protein (Figure S1B). Finally, the novel *S. mansoni* protein has a high degree of similarity (47%) to the other cyclase family members within the "TLED signature domain" (*12*) that contains residues which localize to the active site pocket (Figure S1B). Based on these data, we felt confident that the novel *S. mansoni* gene likely encoded a protein that would fall into the ADP-ribosyl cyclase family of enzymes and would utilize NAD-$(P)^+$ as its substrate. Therefore, we provisionally named the new gene and protein $NAD(P)^+$ catabolizing enzyme or NACE.

We then used the nucleotide and amino acid sequence from NACE to search the public databases to identify any potential NACE orthologues. During the time between our two database searches, a transcriptosome analysis for the related trematode, *S. japonicum*, was published and a clone with significant homology to NACE and the mammalian cyclase CD38 was reported (Accession No. AY222890 (*47*)). In fact, the degree of identity between the amino acid sequence of *S. mansoni* NACE and *S. japonicum* NACE was greater than 56% and the sequences were 74% similar (Figure S2), suggesting that this protein likely represents the *S. japonicum* NACE orthologue. Next, we compared the two NACE sequences to all of the other cyclase family members in order

to generate a phylogram. As shown in Figure 1A, NACE is most closely related to the *Aplysia* cyclases and then to the mammalian cyclase CD157. Since the three-dimensional structures for both the *Aplysia* cyclase and CD157 have been previously published (*6, 14*), we used these structures to model, by homology, the structure of NACE and its putative active site. As shown in Figure 1B, the modeled structure for NACE was very similar to that of CD157, particularly within the substrate-binding groove. Our model also predicts that the highly conserved residues found within the active site of all of the known cyclases, including the catalytic Glu^{202} (*12*), the Glu^{124} of the "signature domain" that regulates hydrolase activity (*13*), and the Trp^{165} that influences substrate positioning (*12*), are localized within the active site pocket of NACE (Figure 1C). However, at odds with the other cyclases, *S. mansoni* NACE has a histidine residue at position 103, while the equivalent position in all other cloned cyclases is invariably occupied by tryptophan, a residue that plays a role in substrate binding within the active site (*12*). Interestingly, the histidine residue in *S. mansoni* NACE is also located within the active site groove of our model (Figure 1C) and is conserved in *S. japonicum* NACE (Figure S2). Taken together, the data indicate that NACE is found in at least two members of the Platyhelminthes phylum, that the amino acid sequence of NACE shares a significant degree of homology with other cyclase family members, and that the predicted structure of the NACE protein is strikingly similar to the other cyclase family members.

Recombinant NACE Is a GPI-Anchored Membrane NAD^+ Glycohydrolase. To determine whether NACE is a functional enzyme we first developed a heterologous (mammalian) in vitro expression system for NACE. Since preferred codon usage between schistosomes and mammals is quite different, we resynthesized the *S. mansoni* NACE cDNA to facilitate translation in mammalian cells (NACE-opt). We then transiently expressed NACE-opt in COS-7 cells and measured NAD^+ glycohydrolase (NADase) activity in the supernatant or cell lysates by measuring the hydrolysis of $1,N^6$-etheno-NAD^+ (ϵ-NAD^+). Hydrolysis of ϵ-NAD^+ by cyclase family members results in the generation of fluorescent ϵ-ADPR that can easily be detected using a spectrofluorometer (ref *55*, see Materials and Methods). We first measured NADase activity in the supernatant of the transfected cells since analysis of the NACE sequence using different protein structure prediction programs (*50, 51*) indicated that NACE had a signal sequence (Figure S2) but no obvious transmembrane domain and would therefore be secreted. However, we did not detect any NADase activity in the transfected cell culture media (Figure 2A), suggesting that NACE may not be secreted. To test this possibility, we lysed the transiently transfected cells in 1% Triton X-100 and then measured NADase activity in the cell lysate. Interestingly, we detected abundant NADase activity in the lysate of COS-7 cells transfected with NACE-opt (Figure 2A), but observed no activity in cells transfected with the empty expression vector (data not shown). These results strongly suggested that NACE is expressed as either a transmembrane or cytosolic protein.

To determine the subcellular localization of NACE, we needed to be able to directly visualize NACE within cells. To facilitate this, we replaced the 5′ signal sequence of
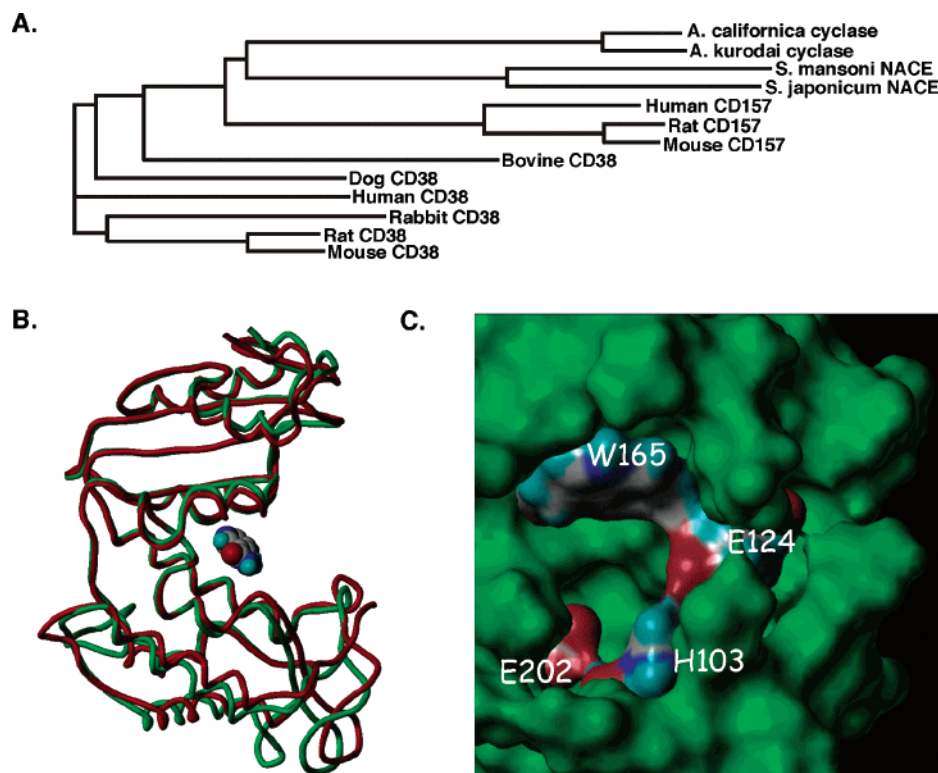
FIGURE 1: NACE is a highly conserved protein expressed by two *Schistosoma* species. (A) Phylogenetic comparison of cyclase family members. The amino acid sequences of the 11 previously identified members of the cyclase family were compared to the two novel NACE sequences and assembled into a phylogenetic tree. (B) Proposed three-dimensional structure of NACE. A homology model was constructed based on the crystallographic coordinates of both *Aplysia* ADP-ribosyl cyclase (PDB entry 1lbe) and human CD157 (PDB entry 1isf) using Modeller (*49*) and energy minimization using AMBER 5.0. A ribbon representation of monomeric NACE (green) is superimposed over that of human CD157 (red). The nicotinamide bound to CD157 (PDB entry 1ism) is shown as space filling model. Carbon atoms are colored in white, oxygen atoms in red, nitrogen atoms in dark blue, and hydrogen atoms in cyan. (C) Connoly surface of the putative active site of NACE. The surfaces of four important amino acids are highlighted using the color code defined in panel B. The amino acid residues shown include the putative catalytic Glu[202], the Glu[124] that regulates the ADP-ribosyl cyclase activity of CD38, and the substrate-binding Trp[165] and His[103]. The rendering was performed using SYBYL (Tripos Inc.).

NACE-opt with a mammalian signal sequence (CD8α leader) followed by a FLAG tag (CD8L/FLAG-NACE). To assess whether the FLAG-tagged recombinant protein could be detected and purified with anti-FLAG reagents, we transiently transfected COS-7 cells with the CD8L/FLAG-NACE construct, lysed the cells in detergent, and purified NACE over an anti-FLAG affinity column. We eluted the FLAG-tagged NACE, separated the purified protein on SDS−PAGE and then performed a Western blot using an anti-FLAG antibody. A protein of approximately 48 kDa was detected in transfected cell lysates (Figure 2B). Next, to determine where NACE was localized in the transfected cells, we transiently transfected COS-7 cells with the CD8L/FLAG-NACE construct and then used a biotinylated anti-FLAG antibody to perform immunofluorescence analysis. As shown in Figure 2C, the plasma membrane of COS-7 cells that were transfected with CD8L/FLAG-NACE specifically stained with the anti-FLAG antibody, while no staining was observed in cells that were transfected with an empty expression vector (Figure 2D). Therefore, these data indicate that NACE, at least when expressed in mammalian cells, is membrane-associated.

These results were somewhat surprising as NACE was not predicted to have a transmembrane domain by any of the commonly used protein structure prediction programs. However, CD157, the closest mammalian relative of NACE, is a membrane-associated GPI-anchored protein. Therefore, we reexamined the C-terminal amino acid sequence of NACE to see if we could identify a GPI anchor motif. Although the NACE C-terminal sequence did not conform with most of the motifs that have been described for mammalian GPI anchors (*61*), we did identify a potential GPI-anchor site (ω-site, see Figure S2) with the help of an algorithm written by Eisenhaber et al. (*52*). To determine whether NACE is GPI anchored, we next tested whether NACE can be cleaved from the membrane of CD8L/FLAG-NACE transfected COS-7 cells by phosphatidylinositol-specific phospholipase C (PI-PLC), a GPI-anchor lipase. We removed the media from transfected and nontransfected COS-7 cells, washed the cells, and then incubated the cells in the presence or absence of PI-PLC. We collected the supernatant 2 h later and measured NADase activity using ϵ-NAD$^+$ as a substrate. As expected, we did not detect NADase activity in the supernatant of cells transfected with the empty vector, regardless of whether PI-PLC was added (Figure 2E). Likewise, we did not detect any activity in the supernatant of cells transfected with CD8L/FLAG-NACE and incubated in media alone (Figure 2E). In contrast, we observed abundant NADase activity in the supernatant collected from the CD8L/FLAG-NACE transfected cells that were incubated with PI-PLC (Figure 2E). Identical results were observed when we performed the experiment using COS-7 cells transfected with the original native form of NACE (data not shown). Thus, NACE, like CD157, is expressed as a GPI-anchored membrane-associated protein in mammalian cells.

NACE Is a Multifunctional Enzyme. Cyclases are multifunctional enzymes that catalyze several reactions including
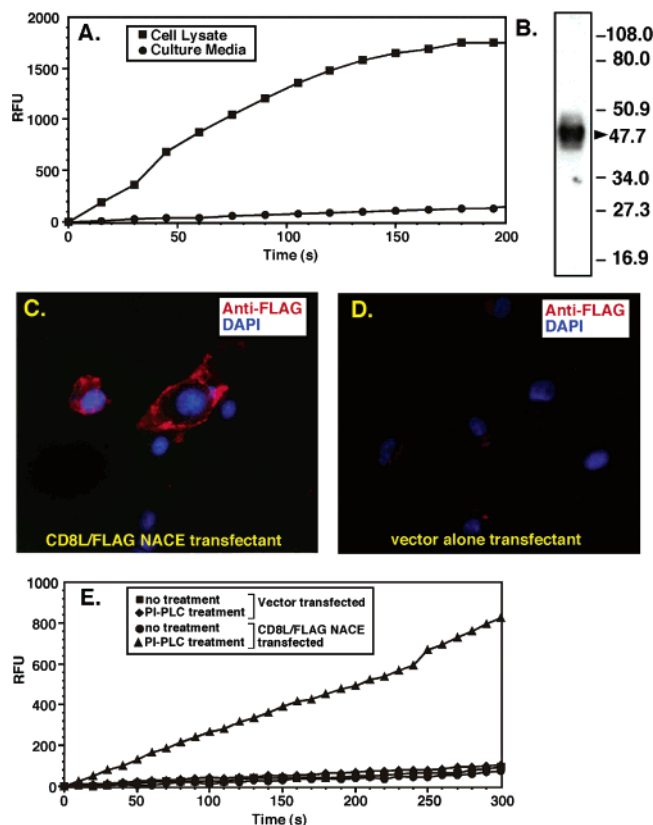
FIGURE 2: *S. mansoni* NACE is a GPI-anchored NADase when heterologously expressed in mammalian cells. (A) Native NACE is cell-associated. COS-7 cells were transiently transfected with the full length NACE (NACE-opt). After 3 days, the culture media (circles) and cells were collected separately. The cells were lysed, and the detergent soluble proteins were collected (squares). Aliquots of the cell lysate and the conditioned tissue culture media were incubated with ϵ-NAD$^+$, and conversion of ϵ-NAD$^+$ to fluorescent ϵ-ADPR was measured over time in a microplate fluorometer. Data are represented in relative fluorescent units (RFU) vs time. No enzyme activity was observed in nontransfected COS-7 cells or COS-7 cells transfected with the empty vector (data not shown). (B) NACE is expressed as a $\sim$48 kDa protein in COS-7 cells. The native signal sequence of *S. mansoni* NACE was replaced with the mammalian CD8 signal sequence and a FLAG tag (CD8L/FLAG-NACE). COS-7 cells were transiently transfected with the CD8L/FLAG-NACE construct, and cell lysates were prepared 3 days post-transfection. The lysates were analyzed by Western blot using an anti-FLAG antibody to identify NACE. (C, D) NACE is expressed as a plasma membrane-associated protein in transfected COS-7 cells. COS-7 cells were transiently transfected on slides with CD8L/FLAG-NACE (panel C) or the empty expression vector (panel D). The transfected cells were fixed and stained with a biotinylated anti-FLAG antibody followed by fluorochrome-coupled streptavidin (red) and a nuclear counterstain (DAPI, blue). Cells were analyzed by fluorescent microscopy. (E) NACE is expressed as a GPI-anchored protein in COS-7 cells. COS-7 cells were transiently transfected with either CD8L/FLAG-NACE (circles and triangles) or the control expression vector (squares and diamonds). Three days later the transfected cells were washed and then cultured in fresh media (squares and circles) or fresh media containing PI-PLC (diamonds and triangles). Two hours later the media were collected and incubated in the presence of ϵ-NAD$^+$. Conversion of ϵ-NAD$^+$ to fluorescent ϵ-ADPR was measured in a microplate fluorometer and is reported as RFU vs time.

the hydrolysis of NAD$^+$ to produce ADPR (NAD$^+$ glyco-hydrolase activity), the cyclization of NAD$^+$ into cADPR (ADP-ribosyl cyclase activity), the hydrolytic conversion of cADPR into ADPR (cADPR hydrolase activity), and the transglycosidation of NADP$^+$ (60). To better characterize

the enzymatic properties of NACE, we produced a secreted soluble form of the NACE ecto-domain by deleting the GPI-anchor motif (see Figure S2) in our FLAG-tagged NACE construct (CD8L/FLAG-NACEΔGPI). We transiently trans-fected COS-7 cells with the new construct, collected the supernatant after 72 h, and measured NADase activity in the supernatant and in the cell lysate using ϵ-NAD$^+$ as a substrate. As expected, the enzyme activity was now highly enriched in the supernatant fraction and was found at only very low levels in the cell lysates (Figure 3A). Next, we purified the secreted NACE protein from the supernatant on an anti-FLAG column and, as expected, affinity purification of NACE resulted in significant enrichment of the NADase activity (Figure 3A, inset). We then analyzed the affinity purified soluble NACE by SDS−PAGE and silver-staining and observed two protein species of 43 and 46 kDa (Figure 3B). To ensure that both of the eluted proteins were bona fide NACE, we performed Western blot analysis using an anti-FLAG antibody. As shown in Figure 3B, both protein species were recognized by the anti-FLAG antibody.

Since we identified two protein forms for NACE and both forms were considerably larger than the predicted molecular weight of soluble NACE ($\sim$30 kDa), we considered the possibility that NACE might be glycosylated, particularly since the NACE sequence contained 4 potential N-linked glycosylation sites (Figure S2). Therefore, we treated the purified recombinant NACE with endoglycosidase F1 (Endo-F) to cleave N-linked sugars and then determined the molecular weight of the treated proteins. Treatment of NACE with Endo-F decreased the size of both forms of NACE by about 2 kDa to 44 and 41 kDa (Figure 3B). Thus, it appears that soluble recombinant NACE is expressed in two isoforms, both of which are N-glycosylated.

Although we easily detected NACE-specific NADase activity using ϵ-NAD$^+$ as a substrate and measuring product formation fluorometrically (i.e., Figure 3A), larger quantities of soluble NACE were needed to better characterize the catalytic properties of NACE. Therefore, we scaled up the production and purification of soluble NACE using a *P. pastoris* expression system and an affinity gel purification scheme that we have routinely employed to purify other cyclases and NAD$^+$ glycohydrolases (62). Similar to what we observed using the mammalian expression system (Figure 3B), we found that soluble NACE is expressed in *Pichia* in two isoforms of 43 and 44 kDa (Figure 3C). We then determined the NAD$^+$ glycohydrolase activity of the purified NACE by incubating the recombinant enzyme with saturating amounts of radiolabeled NAD$^+$ and analyzing product formation by HPLC (Figure 3D). As indicated in Table 1, the specific activity of NACE was calculated to be 13.2 μmol/min/mg of NACE protein, a value that is in the same range as that reported for mammalian cyclases such as CD38 (15, 16, 63). Interestingly, using HPLC to measure product formation, we could easily visualize ADPR but were unable to detect any measurable cADPR (Figure 3D), despite varying the pH of the assay between 5 and 8.0 (data not shown). Since the amount of cADPR produced by NACE was less than the limit of detection by HPLC (i.e., < 1% of the radiolabeled reaction products), we next used a very sensitive cycling assay (57) to measure cADPR production by recombinant soluble NACE. Although we could detect cADPR by this method, the amount produced under steady-
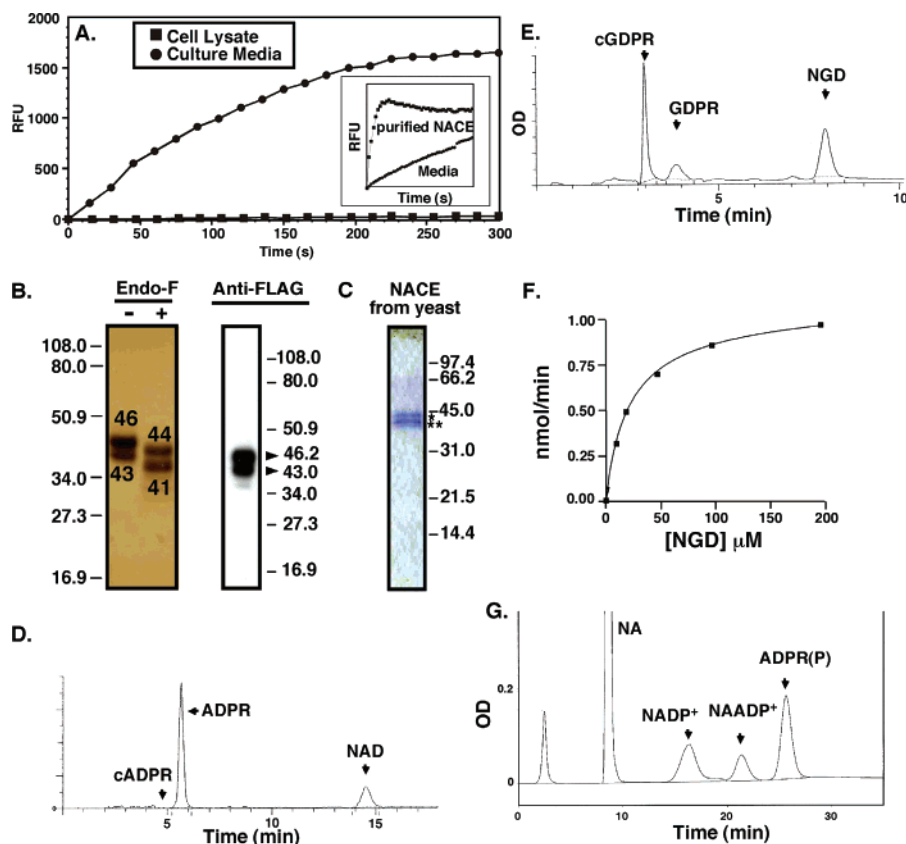
FIGURE 3: Recombinant soluble NACE catalyzes NAD$^+$ glycohydrolase, cyclase, and transglycosidation reactions. (A) Recombinant soluble NACE is secreted. COS-7 cells were transiently transfected with CD8L/FLAG-NACEΔGPI, a construct lacking the GPI anchor sequence. Transfected COS-7 cells were lysed, detergent soluble proteins were collected, and aliquots of the cell lysate (squares) and culture media (circles) were collected. Aliquots were then incubated with ϵ-NAD$^+$, and conversion and accumulation of fluorescent ϵ-ADPR was measured in a microplate fluorometer. The remaining culture medium was purified over an anti-FLAG column, and aliquots were again tested for NADase activity using ϵ-NAD$^+$ as the substrate (inset). Data is reported in RFU vs time. (B) Recombinant soluble NACE is glycosylated in mammalian cells. Recombinant soluble NACE was purified from COS-7 cells transiently transfected with CD8L/FLAG-NACEΔGPI. Affinity purified NACE was incubated in the presence or absence of endoglycosidase-F1 (Endo-F), and the proteins were separated by SDS−PAGE and analyzed by silver staining (left panel) or Western blotting with anti-FLAG antibody (right panel). The molecular weight of soluble recombinant NACE is indicated. (C) Recombinant soluble NACE is expressed in *P. pastoris*. *Pichia* were transformed with an expression vector containing the NACE ecto-domain. A stable clone was selected, and NACE production and secretion were induced with methanol. Secreted NACE was purified from the media by chromatography and analyzed by SDS−PAGE and Coomassie staining. The molecular weights of the purified proteins are 44 (*) and 43 (**) kDa. (D) Soluble recombinant NACE catalyzes the transformation of NAD$^+$ to ADPR. Recombinant soluble NACE was purified from *Pichia* and then incubated with radiolabeled NAD$^+$. The accumulation of radiolabeled ADPR and cADPR was measured by HPLC. (E, F) Soluble recombinant NACE catalyzes the transformation of NGD$^+$ to cyclic GDP-ribose. Purified recombinant soluble NACE was incubated with increasing quantities of NGD$^+$, and the accumulation of cyclic GDPR and GDPR was detected by HPLC and UV detection (260 nm) at various time points. (G) NACE catalyzes the transglycosidation of NADP$^+$ to NAADP$^+$. NADP$^+$ (1 mM) was incubated with recombinant purified NACE at 37 °C in the presence of 20 mM nicotinic acid (NA). Aliquots were analyzed by HPLC as described in Materials and Methods. The compounds were detected by UV absorbance at 260 nm. ADPR(P), adenosine diphosphoribose 2′-phosphate.

Table 1: Kinetic Parameters for the Transformation of Substrates by NACE

substrate[a]	K_m μM	V_{max} μmol/min/mg	k_{cat} s^{-1}	k_{cat}/K_m M^{-1} s^{-1}
NAD$^+$	38.5 ± 6.8	13.2 ± 2.6	6.51 ± 1.28	1.69 × 10^5
NGD$^+$	23.4 ± 1.1	4.8 ± 0.1	2.37 ± 0.05	1.01 × 10^5
NADP$^+$	13.7 ± 2.9	39.2 ± 1.6	19.34 ± 0.79	14.12 × 10^5

[a] All reactions were performed at 37 °C in 10 mM potassium phosphate buffer (pH 7.4) in the presence of purified recombinant NACE produced in *P. pastoris*.

state conditions was very small and represented only 0.016% of the total reaction product ADPR.

These data suggested that either NACE is a much more efficient NAD$^+$ glycohydrolase than ADP-ribosyl cyclase or the produced cADPR is rapidly hydrolyzed by NACE to ADPR (cADPR hydrolase activity). To distinguish between these possibilities, we measured the cADPR hydrolase activity of NACE. We found that NACE is a very poor cADPR hydrolase with an activity of less than 6 nmol/min/mg protein, which is 3 orders of magnitude less than the NAD$^+$ glycohydrolase activity of NACE (Table 1). Therefore, it seemed unlikely that NACE was degrading the cADPR as rapidly as it produced it and more likely that NACE produces very little cADPR under steady-state conditions. To specifically test whether NACE is competent to catalyze a cyclase reaction, we incubated the purified enzyme with NGD$^+$, an analogue of NAD$^+$, which is efficiently converted to the fluorescent product cyclic GDP-ribose (cGDPR) by many of the mammalian cyclase family members (*56*). NGD$^+$ proved to be an excellent substrate for NACE (K_m = 23.4 μM, Table 1) and as shown in Figure 3E was quite efficiently cyclized. The cyclization/hydrolysis ratio was approximately 6.0 (Figure 3E), and the specific

Table 2: Comparison of NACE Enzyme Properties with Cyclase Family Members

properties	NACE	mammalian cyclases	*Aplysia* cyclase
hydrolysis of NAD^+	yes	yes	very low
formation of cADPR	very low	low	yes
hydrolysis of cADPR	very low	yes	very low
formation of cGDPR	yes	yes	yes
transglycosidation	yes	yes	yes
sensivity to INH	no	yes/no	unknown
methanolysis of NAD^+	yes	yes	very low
inhibition by araF-NAD^+	weak ($IC_{50} >$ 10 μM)	K_i nM range	weak ($IC_{50} >$ 10 μM)

activity under steady-state conditions was 4.8 μmol/min/mg protein (Figure 3F, Table 1), all of which is quite comparable to that reported for mammalian cyclases such as CD38 (*63*). Thus, these data show that, while NACE is a very inefficient ADP-ribosyl cyclase, this enzyme is mechanistically competent to catalyze the production of cyclic compounds such as cGDPR.

Next, we tested whether NACE was able to use $NADP^+$ as substrate and to catalyze a transglycosidation reaction in the presence of nicotinic acid. As indicated in Table 1, $NADP^+$ proved to be an excellent substrate of NACE and, in terms of catalytic efficiency (k_{cat}/K_m), $NADP^+$ was an even better substrate than NAD^+ (8-fold better). This is in contrast with human CD38 for which NAD^+ was the favored substrate (*63*). As shown by HPLC (Figure 3G), the pyridine-base exchange reaction was readily catalyzed by NACE, at pH 6.0, indicating that this enzyme, like CD38 and the *Aplysia* cyclase, is able to synthesize the Ca^{2+}-mobilizing messenger $NAADP^+$. As noted before for the other members of the cyclase family, the formation of $NAADP^+$ was less efficient under neutral pH conditions compared to more acidic pH conditions (3-fold reduction in $NAADP^+$ formation at pH 7.4. compared to pH 6.0, data not shown).

In addition to catalyzing a base-exchange reaction using $NADP^+$ as the substrate, we found that NACE can also catalyze a base-exchange reaction using NAD^+ as the substrate in the presence of isoniazid (INH, not shown). This pyridine has been widely used to classify the mammalian NAD^+ glycohydrolases (Table 2) into either "INH-sensitive" (e.g., bovine CD38) or "INH-insensitive" (e.g., human CD38) NADases (*64*), and NACE appears to be a member of the latter category of NADases.

Finally, like the other members of the cyclase family, NACE can catalyze the methanolysis of NAD^+ leading to the formation of β-methyl ADP-ribose (Table 2). On a molar basis, methanol was found to react about 5-fold faster than water (H.M.-S. and F.S., unpublished). Moreover, the presence of 1-3 M methanol did not affect the overall turnover rate of the NAD^+ solvolysis reactions (hydrolysis and methanolysis). These data are consistent with the cleavage of the nicotinamide-ribose bond being the rate-limiting step of the kinetic mechanism of NACE, again similar to what has been previously shown for other cyclase family members such as CD38 (*15, 62, 65*). Taken altogether, the data indicate that the enzymatic properties of NACE are similar to those of other members of the cyclase family (summarized in Table 2), and that NACE can catalyze the production of ADPR and $NAADP^+$. However, despite being competent to catalyze a cyclase reaction, NACE is a highly inefficient ADP-ribosyl
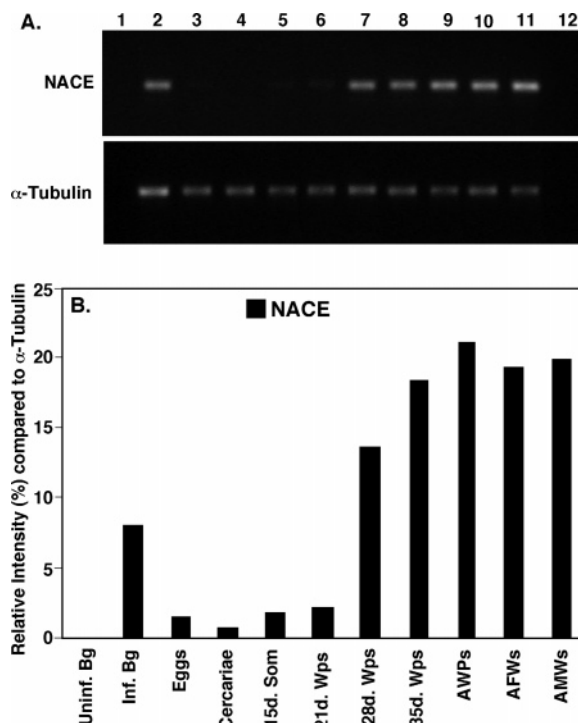

FIGURE 4: NACE expression is developmentally regulated in *S. mansoni*. (A) cDNA prepared from RNA isolated from multiple developmental stages of *S. mansoni* was used as templates for RT-PCR reactions using NACE-specific primers. Schistosome specific α-tubulin primers were used to amplify a constitutively transcribed internal control gene. Tested stages are numbered from 1 to 12, and they represent the following: uninfected *B. glabrata*, 30-day infected *B. glabrata*, *S. mansoni* eggs, *S. mansoni* cercariae, *S. mansoni* 15-day schistosomules, 21-day schistosomules, 28-day worms, 35-day worms, adult (>42-day old) worm pairs, adult female worms, adult male worms and no reverse transcriptase (−RT) control, respectively. (B) Bar-graph representation of the average expression level of NACE exhibited by each tested developmental stage of the parasite life cycle as percentage of levels of α-tubulin internal control. Data shown are averages of values quantified from three independent PCR amplifications. Background (−RT control) was subtracted from each of the analyzed samples.

cyclase and makes only trace amounts of cADPR under steady-state conditions.

NACE Expression Is Developmentally Regulated in Schistosoma mansoni. Although it was clear that NACE can be expressed as a GPI-anchored ecto-enzyme in mammalian cells, it was not clear when or where NACE is expressed during the life cycle of *S. mansoni*. To address these issues, we first determined when NACE mRNA transcripts are expressed during schistosome development using a semi-quantitative PCR approach with NACE-specific and *S. mansoni* α-tubulin specific primers. We found that NACE transcripts were not detectable in *S. mansoni* eggs or in uninfected *Biomphalaria glabrata* snails (intermediate hosts) but were easily observed in the *S. mansoni*-infected snails (Figure 4A). To our surprise, NACE expression then declined to undetectable levels in the *S. mansoni* cercariae and schistosomules and in immature day 21 worm pairs (Figure 4A,B). In contrast, NACE expression was dramatically increased in day 28 and day 35 worm pairs, coinciding with male−female worm pairing, and was then maintained in both male and female mature adult worm pairs (Figure 4A,B). Together, these data suggest that NACE may play a developmentally regulated signaling function in *S. mansoni* in both intermediate and definitive hosts.
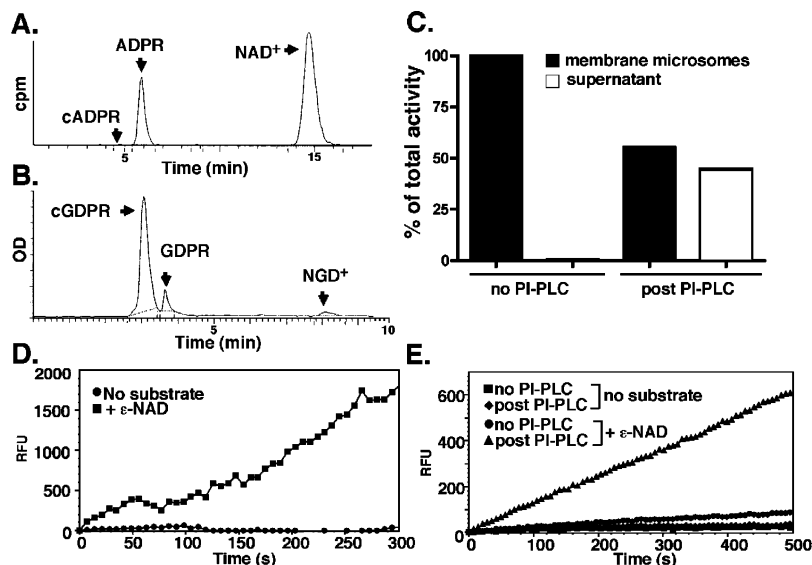
FIGURE 5: Adult *S. mansoni* worms express a GPI-anchored NADase on the outer membrane. (A−C) Adult *S. mansoni* worms express a GPI-anchored NAD⁺ glycohydrolase and NGD⁺ cyclase. Membrane microsomes were prepared from 2 g of frozen adult *S. mansoni* worms. The microsomes were resuspended in buffer and incubated with ¹⁴C-labeled NAD⁺ (A) or unlabeled NGD⁺ (B). Product formation was measured by HPLC as described in Figure 3. In panel C, the membrane microsomes were incubated in the presence or absence of PI-PLC for 2 h. The supernatant and membrane fractions were collected separately and then incubated with ¹⁴C-labeled NAD⁺. ADPR production was measured by HPLC, and results are presented as % activity compared to the nontreated membrane fraction. The specific activity of nontreated membrane microsomes was 36 nmol/min/mg protein. (D) Adult *S. mansoni* worms express an outer membrane NAD⁺ glycohydrolase. Ten live adult *S. mansoni* worms were placed in single wells of a 96 well plate and were incubated in media (circles) or media containing ϵ-NAD⁺ (squares), and conversion of ϵ-NAD⁺ to fluorescent ϵ-ADPR was measured in a microplate fluorometer and is reported in RFU vs time. (E) Adult *S. mansoni* worms express a GPI-anchored outer tegument NADase. Ten live adult *S. mansoni* worms were placed in single wells of a 96 well plate and were then incubated in the presence (diamonds and triangles) or absence (squares and circles) of PI-PLC for 2 h. The medium from each of the wells was removed and then incubated in the presence (circles and triangles) or absence (squares and diamonds) of ϵ-NAD⁺. Production of fluorescent ϵ-ADPR was measured in a microplate fluorometer and is reported as RFU over time.

NACE Is Expressed as a Constitutively Active Ecto-Enzyme in the Tegument Membrane of Adult S. mansoni. To evaluate whether NACE protein is expressed and functional in adult *S. mansoni* worms, we first purified membrane and cytosolic fractions from homogenized adult worms and assessed NAD⁺ glycohydrolase activity using radiolabeled NAD⁺ as a substrate. Identical to our results using the heterologous mammalian expression system, NAD⁺ glycohydrolase activity was observed exclusively in the membrane microsome fraction of the adult *S. mansoni* worms. In addition, despite using the sensitive assay with radiolabeled NAD⁺ as the substrate, we were only able to detect the formation of ADPR, and not cADPR (Figure 5A), suggesting that the native enzyme, like the recombinant version, is a very inefficient ADP-ribosyl cyclase. To test whether the native NACE could catalyze a cyclase reaction, we incubated the membrane microsomes with NGD⁺ and measured cGDPR accumulation fluorometrically and by HPLC. As expected, the *S. mansoni* membrane fraction very efficiently catalyzed a cyclase reaction with a cGDPR/GDPR ratio of 12 (Figure 5B).

Next, to determine whether the membrane-associated NAD⁺ glycohydrolase/NGD⁺ cyclase expressed by adult *S. mansoni* worms was GPI-anchored, we incubated the microsomal fraction in the presence and absence of PI-PLC and then measured NAD⁺ glycohydrolase activity released into the supernatant. As expected, we found that the schistosome NAD⁺ glycohydrolase was sensitive to PI-PLC (Figure 5C). Together, these data indicate that the *Schistosoma* NAD⁺ glycohydrolase is a membrane-associated GPI-anchored protein.

Schistosomes, like all flatworms, have an outer membrane, referred to as the tegument (*66*). The tegument is composed of a syncytium having a heptalaminar apical membrane and a basal membrane separated by 9 nm of cytoplasm connecting via a cytoplasmic bridge to subtegumental cytons. To assess whether the schistosome NAD⁺ glycohydrolase is associated with the outer tegument membrane of the adult worm, we directly incubated live schistosome parasites with the membrane impermeant substrate ϵ-NAD⁺ and measured accumulation of fluorescent ϵ-ADPR. As shown in Figure 5D, as few as 10 live *S. mansoni* adult worms were able to efficiently catalyze the NAD⁺ glycohydrolase reactions, indicating that adult *S. mansoni* parasites express an enzyme-(s) with the properties of NACE on the outer tegument. To determine whether the NADase associated with the outer tegument of *S. mansoni* adult worms is GPI-anchored, we incubated 10 live parasites in the presence or absence of PI-PLC, collected the supernatant after 2 h, and measured NAD⁺ glycohydrolase activity using ϵ-NAD⁺ as the substrate (Figure 5E). As expected, culture media from the worms that were incubated without PI-PLC was devoid of NADase activity, however we easily detected NADase activity in the medium from the worms that were treated with PI-PLC (Figure 5E). Finally, to ensure that we were detecting an authentic NAD⁺ glycohydrolase on the outer tegument and not a pyrophosphatase (which can also utilize ϵ-NAD⁺ as a substrate and generate fluorescent products), we incubated the PI-PLC treated supernatant with 1,N^6-etheno-PyAD⁺, a substrate that is transformed by nucleotide pyrophosphatases into the fluorescent 1,N^6-etheno-AMP, but cannot be utilized by members of the cyclase family (*67*). No pyrophosphatase
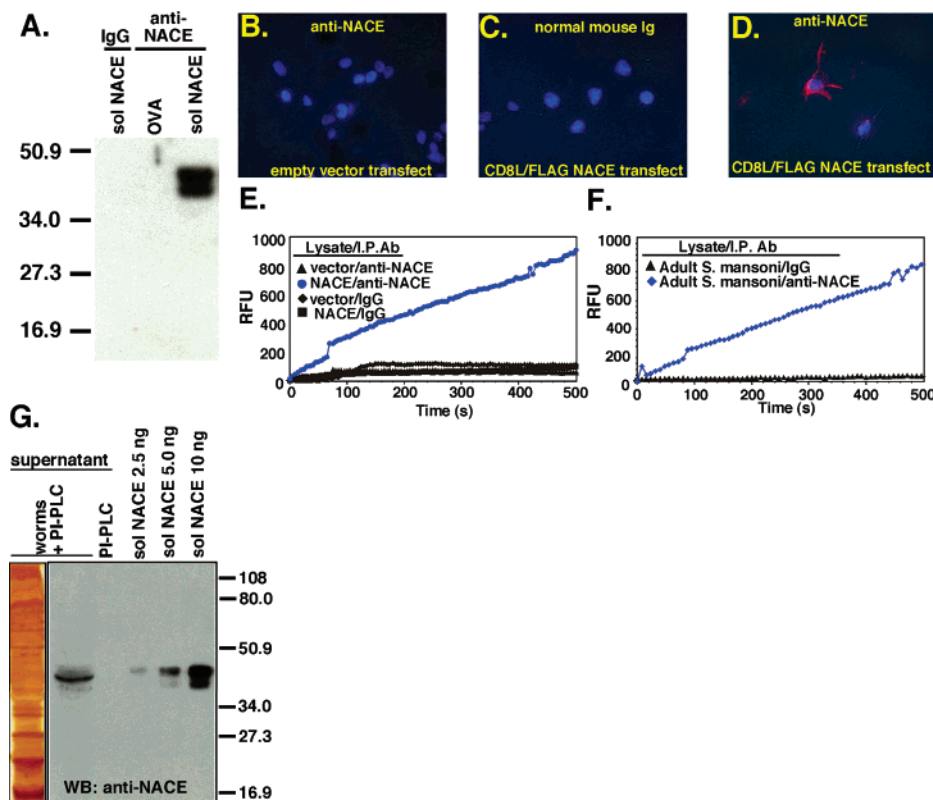
FIGURE 6: Antiserum raised against the NACE cDNA immunoprecipitates enzymatically active NACE from adult *S. mansoni* worms. (A) Antibodies raised in response to NACE cDNA immunization recognize recombinant soluble NACE. Control serum (IgG) and antiserum collected from mice vaccinated with the CD8L/FLAG-NACEΔGPI construct (anti-NACE) were used to probe Western blots containing recombinant soluble NACE or irrelevant protein (ovalbumin, OVA). (B–D) Antiserum raised in response to immunization with NACE cDNAs specifically recognize plasma membrane-associated NACE. COS-7 cells were transiently transfected on slides with CD8L/FLAG-NACE (C, D) or the empty expression vector (B). Three days later the cells were stained with anti-NACE antiserum (B, D) or normal mouse serum (C) followed by fluorochrome coupled anti-mouse IgG (red) and a nuclear counterstain (DAPI, blue). (E) Anti-NACE antibodies immunoprecipitate functional NACE protein from transfected COS-7 cells. COS-7 cells were transiently transfected with CD8L/FLAG-NACE (squares and circles) or the empty expression vector (diamonds and triangles). Three days later the cells were lysed and the lysates were incubated either with normal mouse IgG protein G beads (diamonds and squares) or with anti-NACE protein G beads (triangles and circles). The immunoprecipitated protein/bead complexes were incubated in the presence of ϵ-NAD$^+$, and the accumulation of fluorescent ϵ-ADPR was measured using a microplate fluorometer. Data is reported in RFU vs time. (F) Antibodies raised in response to NACE cDNA immunization immunoprecipitate enzymatically active NACE from adult *S. mansoni* lysates. Adult *S. mansoni* worms were lysed in detergent, and the lysates were incubated either with normal mouse IgG protein G beads (triangles) or with anti-NACE protein G beads (diamonds). The immunoprecipitated protein/bead complexes were incubated in the presence of ϵ-NAD$^+$, and the accumulation of fluorescent ϵ-ADPR was measured using a microplate fluorometer. Data is reported as RFU vs time. (G) Antibodies raised in response to NACE cDNA immunization recognize a GPI-anchored protein expressed by adult *S. mansoni* worms. Live adult worms were incubated in HBSS in the presence of PI-PLC for 2 h. The supernatant was collected, concentrated, and then separated on an SDS−PAGE gel. 15% of the total protein was analyzed by silver staining and Western blot using anti-NACE antiserum. Control lanes include PI-PLC alone and increasing concentrations of recombinant soluble NACE.

activity was detected (data not shown), thus the enzyme present on the outer tegument of adult worms is an authentic GPI-anchored NAD$^+$ glycohydrolase.

Our data suggested that NACE or a NACE-like enzyme is expressed as an outer tegument protein by adult *S. mansoni* worms. To directly test this hypothesis, we generated NACE specific antibodies by performing DNA immunization of mice using the CD8LFLAG-NACEΔGPI expression construct. We collected serum from the immunized mice and assessed the specificity of the antiserum by Western blot, immunofluorescence, and immunoprecipitation. As shown in Figure 6A, the antiserum raised in response to the NACE cDNA vaccine specifically recognized soluble recombinant NACE protein by Western blot but did not react with other purified proteins including ovalbumin. Next, to determine whether the anti-NACE antiserum would specifically recognize membrane-associated NACE protein, we transiently transfected COS-7 cells with CD8L/FLAG-NACE or the

empty expression vector and then stained the cells with the anti-NACE antiserum followed by a fluorochrome-conjugated anti-mouse immunoglobulin antibody. As expected, the anti-NACE antiserum did not stain the empty vector-transfected cells (Figure 6B) nor did normal mouse serum stain NACE-transfected cells (Figure 6C). However, identical to what we observed when we stained the NACE transfected cells with anti-FLAG antibody (see Figure 2C), the anti-NACE antiserum stained the plasma membrane of COS-7 cells transfected with CD8L/FLAG-NACE (Figure 6D).

To demonstrate that the anti-NACE antiserum could be used to immunoprecipitate enzymatically active NACE protein, we transiently transfected COS-7 cells with CD8L/FLAG-NACE or the empty expression vector, lysed the transfected cells in Triton X-100, and collected the detergent soluble proteins. We performed immunoprecipitations using the anti-NACE antiserum or normal mouse serum coupled to protein G beads and then analyzed whether the immuno-

precipitated proteins were able to catalyze the hydrolysis of ϵ-NAD$^+$. No enzyme activity was observed in immunoprecipitates from control transfected cells, regardless of whether normal mouse serum or anti-NACE antiserum was used as the immunoprecipitating antibody (Figure 6E). Likewise, no enzyme activity was detected in the immunoprecipitates using the normal mouse serum and lysates from the NACE-transfected cells (Figure 6E). However, we detected abundant NAD$^+$ hydrolase activity in the immunoprecipitated proteins isolated from the NACE-transfected cells using the anti-NACE antiserum (Figure 6E). Together, these data indicate that the antiserum raised against the NACE cDNA is specific for NACE and recognizes enzymatically active membrane-anchored NACE as well as denatured NACE.

To determine whether enzymatically active NACE protein is expressed by adult *S. mansoni* worms, we lysed adult worms in Triton X-100, collected the detergent soluble proteins, and performed immunoprecipitations using our anti-NACE antiserum or normal mouse serum as a control. We then determined whether the proteins precipitated from the adult worms were able to hydrolyze ϵ-NAD$^+$. As shown in Figure 6F, the anti-NACE immunoprecipitated proteins catalyzed a NAD$^+$ glycohydrolase reaction while the proteins that were immunoprecipitated with normal mouse serum had no detectable enzyme activity.

To visualize the native NACE protein expressed by adult *S. mansoni* worms, we incubated live worms in HBSS in the presence of PI-PLC. We collected and concentrated the proteins released into the culture media and then analyzed the proteins by silver staining and Western blot. As shown in Figure 6G, a large number of proteins were either secreted or shed by the PI-PLC-treated adult worms. However, upon Western blot analysis using our anti-NACE antiserum, a single protein of approximately 43 kDa was detected (Figure 6G). Interestingly, the native NACE protein expressed by the adult *S. mansoni* worms was very similar in size to the soluble recombinant NACE secreted by transfected COS-7 cells (Figure 6G). Native NACE was also detected as two similar-sized proteins using anti-NACE antibodies to probe Western blots of extracts isolated from live worms treated with NP-40 to enrich for surface-associated proteins (Supporting Information Figure S3). Taken together these data show that an antiserum raised against NACE, a novel protein encoded by a cDNA isolated from *S. mansoni*, specifically recognizes a surface-associated GPI-anchored protein in adult *S. mansoni* worms that is capable of catalyzing NAD$^+$ glycohydrolase and NGD$^+$ cyclase reactions.

Finally, RT-PCR data and Western blot experiments using anti-NACE antibodies strongly suggested that NACE is developmentally expressed as a membrane- and tegument-associated protein in adult *S. mansoni* parasites. To confirm these findings, we used the IgG fraction of the anti-NACE antiserum to detect the native NACE protein in adult worm cryosections, whole mount worms, and mechanically transformed schistosomules (Figure 7). As expected based on the PCR expression data, NACE protein was not detected in either live or acetone-fixed 3 h schistosomules (data not shown). Similarly, no specific fluorescence was observed in adult worm cryosections (Figure 7C) or whole worms (Figure 7G) when probed with preimmune normal mouse IgG. In contrast, strong surface staining along the male gynecophoric canal (arrow; Figure 7F) as well as fluorescence of the

epithelial tissues surrounding the gut (not shown) could be seen in adult worm cryosections probed with anti-NACE antibody. In addition, surface fluorescence was also detected in acetone-fixed (Figure 7H) or live (Figure 7I) whole worms probed with anti-NACE antibodies. Specific staining was observed on the surface (tubercles, Figure 7H), male gynecophoric canal (Figure 7H), and oral and ventral suckers of male and female worms (Figure 7H,I). Thus, these data indicate that in adult schistosomes NACE is localized to the outer surface of the parasite. The implications of these results for potential NACE-based vaccines and small molecule antagonists are discussed.

DISCUSSION

Cyclic ADP-ribose is considered to be a ubiquitous Ca^{2+}-mobilizing second messenger as it can mediate calcium release in a large variety of cell types isolated from organisms that represent three different kingdoms including plants, animals, and protists (*60*). This suggests that the enzyme(s) that catalyze the production of cADPR from NAD$^+$ would likely be equally well conserved and found in most species. Indeed, the original members of the ADP-ribosyl cyclase family of enzymes were cloned from the gastropod *A. californica*, and other family members were soon identified in a variety of different mammalian species. These enzymes were clearly family members as the intron/exon structure of the genes was very similar (*68*), the critical structural domains were absolutely conserved (*6, 12, 14*), and all of the family members were competent to catalyze a cyclase reaction, albeit with differing efficiencies (*15*).

We have now identified a new member of the ADP-ribosyl cyclase family, NACE, which is present in at least two species of *Schistosoma*. NACE is clearly a member of this family of enzymes in that the critical cysteine residues required for the tridimensional structure (*6, 14*) are conserved and the catalytic and a key substrate-binding residue (*12*) are present. Furthermore, our structure modeling predicts that the substrate binding and catalytic residues will be located within the active site pocket of NACE. The data also clearly demonstrate that NACE is a constitutively active NADase whether expressed in its native form in adult *S. mansoni* parasites or in transfected mammalian cells. A direct comparison of NACE enzyme properties with other cyclase family members is shown in Table 2. Identical to the other cyclase family members, both recombinant and native NACE can hydrolyze NAD$^+$ and produce ADPR, a known activator of the mammalian plasma membrane ion channel TRPM2 (*32−34*). NACE can also catalyze a base-exchange reaction between NADP$^+$ and nicotinic acid to produce detectable quantities of NAADP$^+$, a known activator of intracellular Ca^{2+} release in many cell types (*60*).

Although NACE is able to catalyze ADP-ribosyl cyclase reactions using NAD$^+$ as a substrate, the schistosome enzyme is far less efficient at catalyzing this reaction compared to other members of this family of enzymes (Table 2). In fact, it was not possible to detect cADPR production by either soluble recombinant NACE or native membrane-associated NACE, despite using a sensitive assay with [^{14}C]NAD$^+$ as the substrate and detecting the radiolabeled products separated by HPLC. It was not until we switched to the very sensitive cycling assay (*57*) that we were able to conclude that NACE was able to produce cADPR, albeit in extremely
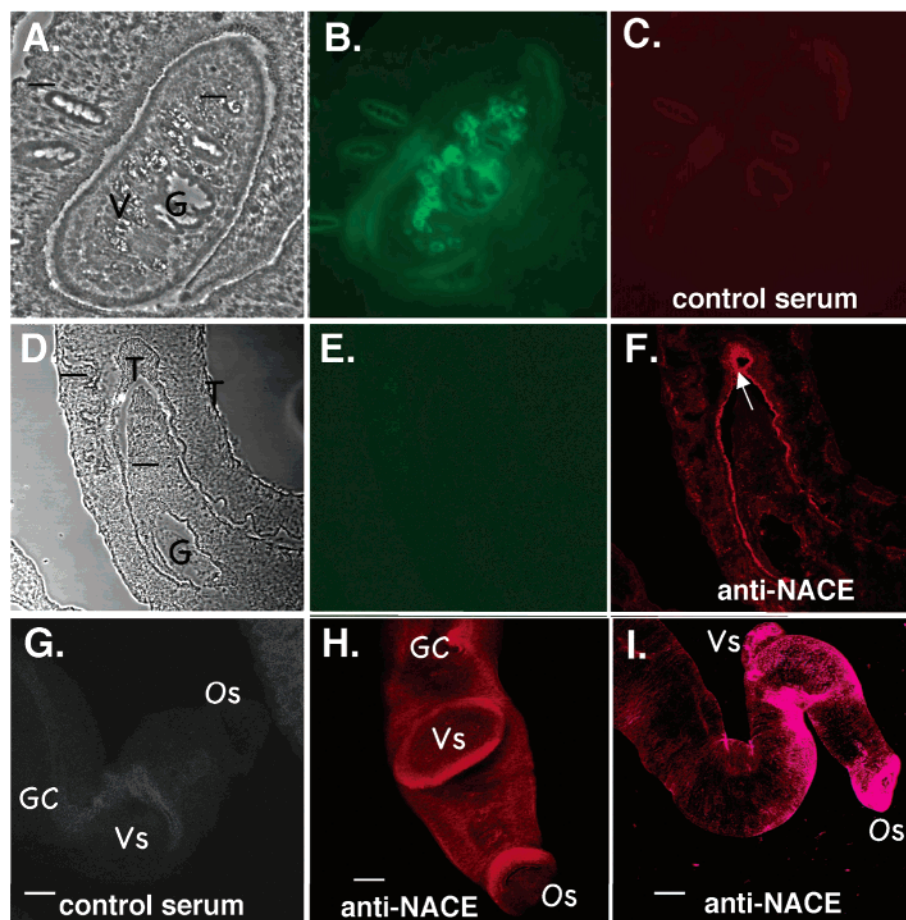
FIGURE 7: Immunohistochemical localization of NACE in adult *S. mansoni*. Adult schistosome cryosections (A—F) and live or acetone-fixed whole-mount adult worms (G—I) were prepared. Panels A and D represent phase contrast fields. Samples visualized using a green fluorescence filter (panels B and E) indicate autofluorescent structures including female worm vitellaria (panel B). To localize NACE, sections and whole mounts were probed with the IgG fraction purified from the anti-NACE antiserum (panels F, H, I) or with normal mouse IgG (panels C, G) followed by biotinylated anti-mouse IgG and Alexa Fluor 647 conjugated streptavidin. NACE was visualized using a far-red fluorescence filter (650 nm). Slides stained with normal mouse IgG did not show any specific reactivity (panel C, G), while slides stained with anti-NACE antibody showed specific staining in the tegument layer of male worm gynecophoric canal (arrow, panel F). Acetone-fixed whole adult worms (male worm shown) stained with anti-NACE mouse IgG showed strong overall fluorescence (panel H), while in live whole worms (female shown, panel I) fluorescence was more localized to oral sucker (Os), ventral sucker (Vs), and tubercles (Tu). V stands for vitellaria, G is gut, T is tegument, and GC is male gynecophoric canal. Sections and whole worms were photographed at 200× and 100× magnifications, respectively.

limited amounts (i.e., less than 0.02% of reaction products). The low accumulation of cADPR in the reaction is not due to rapid hydrolysis of cADPR to ADPR by NACE as the cADPR hydrolase activity of NACE is also very low. We considered the possibility that NACE activity might be pH sensitive, as it is known that CD157 is a much more efficient cyclase under lower pH conditions (*20*), but despite varying the pH of the reaction between pH 5.0 and pH 8.0, we were still unable to detect production of radiolabeled cADPR by HPLC. However, we know that NACE is competent to catalyze a cyclase reaction as it can efficiently cyclize NGD^+ to cGDPR. Thus, while NACE is clearly a member of the cyclase family from a structural standpoint, functionally it is unusual as it cannot efficiently produce the signature metabolite, cADPR.

Interestingly, CD38 and CD157, although clearly better at producing cADPR than NACE, are still relatively inefficient cyclases when compared to the *Aplysia* cyclases (*15, 16*). Instead, CD38 and CD157 were shown to primarily produce ADPR (*15, 16*). Detailed kinetic analysis revealed that all the cyclases follow a partition mechanism. Accordingly after binding NAD^+, they catalyze the cleavage of the

nicotinamide—ribose bond to form an E·ADP-ribosyl reaction intermediate within the active site pocket of the enzyme (*62, 69—71*). This reactive intermediate then partitions following competing pathways; it either is cyclized to form cADPR (cyclase reaction) or, if H_2O can gain entry to the active site, is hydrolyzed to irreversibly form ADPR (NAD^+ glycohydrolase reaction). In the case of the *Aplysia* cyclase, the active site appears to largely exclude the entry of H_2O and the cyclization reaction is more favored, while in the case of the mammalian cyclases, the active site is more accessible to H_2O allowing hydrolysis to occur (*15*).

Our data argue that NACE also shares the mechanistic signature of cyclases and must form a reactive E·ADP-ribosyl intermediate that can partition between different acceptors such as water and pyridines (intermolecular reactions) or N1 or N7 of the adenine and guanine rings of NAD^+ and NGD^+ respectively (intramolecular reactions) (*15*). In NACE, however, the reactivity of N1 of the adenine ring leading to the formation of cADPR is even lower than in the other cyclases such as CD38. This might result from the positioning/orientation of the adenine ring within the substrate binding domain of NACE and is likely to be inherent to the

structure and topology of the active site of this enzyme which is slightly different from that of other cyclases, particularly at sites of contact between the enzyme and substrate (Figure 1C).

If NACE does not mediate its biologic activity by producing cADPR, then we are left with the question of what functional role this enzyme might play in adult schistosomes. It is well-known that tight regulation of Ca^{2+} flux across the tegument of adult schistosomes is necessary for the long-term viability of the worm. Indeed, the most effective drug to treat schistosomiasis is Praziquantel, a compound that apparently works by inducing a rapid Ca^{2+} flux across the tegument into the worm, leading to muscle contraction and subsequent "paralysis" of the worm (72−74). Therefore, one potential role that NACE may play is to mediate Ca^{2+} signaling in schistosomes by producing ADPR or $NAADP^+$. ADPR, at least in mammalian cells, is known to regulate Ca^{2+} influx across the plasma membrane by binding to the nudix motif on the transient receptor potential channel TRPM2 (32−34), while $NAADP^+$ mediates intracellular Ca^{2+} release through RyRs in mammalian cells (27−31). Interestingly, smooth muscle fibers isolated from disassociated adult *S. mansoni* worms express RyRs that release Ca^{2+} in response to ryanodine (75, 76) and undergo contraction in response to RyR agonists such as caffeine (77). Schistosomes are also known to express voltage-gated calcium channels (78) and express a cDNA with weak similarity to human TRPC3 (TIGR *S. mansoni* GenBank Accession No. CD181297), another member of the transient receptor potential channel family. Thus, despite producing very limited amounts of cADPR, NACE may still play an important role in regulating Ca^{2+} responses in adult schistosomes.

Alternatively, NACE may play a more important role in regulating ecto-NAD^+ levels in the host. Since NACE is expressed on the outer tegument of the adult worm, access to substrate appears to be limited to extracellular NAD^+ which is also the source of substrate for CD38 and CD157 as well as the mono-ADP-ribosyl transferases such as ART2 (79, 80). Therefore, it is possible that one function of NACE may be to catabolize extracellular NAD^+ and thereby "inhibit" the mammalian NADases by reducing substrate availability. Since CD38, CD157, and ART2 have all been shown to regulate the effector functions of lymphocytes (38, 39, 80, 81), NACE may function as an immune evasion or immunosuppressing molecule in the adult parasite. This is plausible as adult schistosomes have been shown to be the least susceptible stage to immune elimination and to have evolved mechanisms of immune evasion (82). In the future it will be important to test whether extracellular NAD^+ levels are decreased in *Schistosoma*-infected hosts and whether this alters the function of other NADases such as CD38.

Finally, it will be interesting to determine whether specific small molecule antagonists of NACE can be used either to alter extracellular NAD^+ homeostasis or to alter Ca^{2+} signaling in the adult schistosome. Since the induced expression of NACE corresponds with the mating of the male and female schistosomes in the portal circulation of the liver, it is possible that NACE regulates the viability, mating, fertilization of the eggs, or even trafficking of the adult worms within the mammalian host. Importantly, our data indicates that the structures of the active sites of NACE and

the mammalian cyclases are somewhat different, which may facilitate the identification of NACE-specific antagonists or inhibitors. In fact, we have recently tested the effect of nicotinamide 2′-deoxy-2′-fluoroarabinoside adenine dinucleotide (araF-NAD^+) on NACE enzyme activity. This NAD^+ analogue, which is one of the most potent inhibitors of CD38, behaves as a slow-binding inhibitor with a K_i in the low nM range (63, 83). Interestingly, incubation of NACE with up to 10 μM araF-NAD^+ did not show an inhibition pattern and only resulted in a 25% reduction in enzyme activity (Table 2), indicating that araF-NAD^+ is at best a very weak and classical inhibitor of NACE. Most importantly, the data suggest that it should be possible to identify small molecules that specifically target the subtle differences between the active sites of NACE and other cyclases such as human CD38.

In conclusion, we have identified and characterized NACE, a new member of the ADP-ribosyl cyclase family of enzymes in the Platyhelminthes trematodes, *S. mansoni* and *S. japonicum*. NACE is a highly unusual and novel member of the family that does not produce significant quantities of the signature metabolite, cADPR. However NACE can catabolize extracellular $NAD(P)^+$ to produce at least two different known Ca^{2+}-mobilizing metabolites, ADPR and $NAADP^+$, and therefore has the potential to regulate Ca^{2+}-dependent signaling as well as ecto-NAD^+ homeostasis. In addition, given that NACE expression is developmentally regulated and restricted to the outer tegument of the adult schistosome, it can be the target of both vaccination and small molecule antagonists/inhibitors, making it an ideal candidate for vaccine development and drug discovery.

SUPPORTING INFORMATION AVAILABLE

The complete cDNA sequence of NACE (Figure S1), the amino acid comparison between *S. mansoni* and *S. japonicum* NACE and other members of the ADP-ribosyl cyclase family members (Figures S1 and S2), and Western blot analysis of NACE expression in *S. mansoni* extracts (Figure S3). This material is available free of charge via the Internet at http://pubs.acs.org.

REFERENCES

1. Lee, H. C., Walseth, T. F., Bratt, G. T., Hayes, R. N., and Clapper, D. L. (1989) Structural determination of a cyclic metabolite of NAD^+ with intracellular Ca^{2+}-mobilizing activity, *J. Biol. Chem. 264*, 1608−1615.
2. Hellmich, M. R., and Strumwasser, F. (1991) Purification and characterization of a molluscan egg-specific NADase, a second-messenger enzyme, *Cell. Regul. 2*, 193−202.
3. Lee, H. C., and Aarhus, R. (1991) ADP-ribosyl cyclase: an enzyme that cyclizes NAD^+ into a calcium mobilizing metabolite, *Cell Regul. 2*, 203−209.
4. Glick, D. L., Hellmich, M. R., Beushausen, S., Tempst, P., Bayley, H., and Strumwasser, F. (1991) Primary structure of a molluscan egg-specific NADase, a second-messenger enzyme, *Cell Regul. 2*, 211−8.

5. Nata, K., Sugimoto, T., Tohgo, A., Takamura, T., Noguchi, N., Matsuoka, A., Numakunai, T., Shikama, K., Yonekura, H., Takasawa, S., et al. (1995) The structure of the Aplysia kurodai gene encoding ADP-ribosyl cyclase, a second-messenger enzyme, *Gene 158*, 213−218.

6. Prasad, G. S., McRee, D. E., Stura, E. A., Levitt, D. G., Lee, H. C., and Stout, D. C. (1996) Crystal structure of *Aplysia* ADP ribosyl cyclase, a homologue of the bifunctional ectoenzyme CD38, *Nature Struct. Biol. 3*, 957−964.

7. Harada, N., Santos-Argumedo, L., Chang, R., Grimaldi, J. C., Lund, F. E., Brannan, C. I., Copeland, N. G., Jenkins, N. A., Heath, A. W., Parkhouse, R. M. E., and Howard, M. (1993) Expression cloning of a cDNA encoding a novel murine B cell activation marker, *J. Immunol. 151*, 3111−3118.

8. Jackson, D. G., and Bell, J. I. (1990) Isolation of a cDNA encoding the human CD38 (T10) molecule, a cell surface glycoprotein with an unusual discontinuous pattern of expression during lymphocyte differentiation, *J. Immunol. 144*, 2811−2815.

9. Kaisho, T., Ishikawa, J., Oritani, K., Inazawa, J., Tomizawa, H., Muraoka, O., Ochi, T., and Hirano, T. (1994) BST-1, a surface molecule of bone marrow stromal cell lines that facilitates pre-B-cell growth, *Proc. Natl. Acad. Sci. U.S.A. 91*, 5325−5329.

10. Itoh, M., Ishihara, K., Tomizawa, H., Tanaka, H., Kobune, Y., Ishikawa, J., Kaisho, T., and Hirano, T. (1994) Molecular cloning of murine BST-1 having homology with CD38 and *Aplysia* ADP-ribosyl cyclase, *Biochem. Biophys. Res. Commun. 203*, 1309−1317.

11. Dong, C., Wang, J., Neame, P., and Cooper, M. D. (1994) The murine BP-3 gene encodes a relative of the CD38/NAD glycohydrolase family, *Int. Immunol. 6*, 1353−1360.

12. Munshi, C., Aarhus, R., Graeff, R., Walseth, T. F., Levitt, D., and Lee, H. C. (2000) Identification of the enzymatic active site of CD38 by site-directed mutagenesis, *J. Biol. Chem. 275*, 21566−21571.

13. Graeff, R., Munshi, C., Aarhus, R., Johns, M., and Lee, H. C. (2001) A single residue at the active site of CD38 determines its NAD cyclizing and hydrolyzing activities, *J. Biol. Chem. 276*, 12169−12173.

14. Yamamoto-Katayama, S., Ariyoshi, M., Ishihara, K., Hirano, T., Jingami, H., and Morikawa, K. (2002) Crystallographic studies on human BST-1/CD157 with ADP-ribosyl cyclase and NAD glycohydrolase activities, *J. Mol. Biol. 316*, 711−723.

15. Schuber, F., and Lund, F. E. (2004) Structure and enzymology of ADP-ribosyl cyclases: Conserved enzymes that produce multiple calcium mobilizing metabolites, *Curr. Mol. Med. 4*, 249−261.

16. Howard, M., Grimaldi, J. C., Bazan, J. F., Lund, F. E., Santos-Argumedo, L., Parkhouse, R. M. E., Walseth, T. F., and Lee, H. C. (1993) Formation and hydrolysis of cyclic ADP-ribose catalyzed by lymphocyte antigen CD38, *Science 262*, 1056−1059.

17. Takasawa, S., Togho, A., Noguchi, N., Koguma, T., Nata, K., Sugimoto, T., Yonekura, H., and Okamoto, H. (1993) Synthesis and hydrolysis of cyclic ADP-ribose by human leukocyte antigen CD38 and inhibition of the hydrolysis by ATP, *J. Biol. Chem. 268*, 26052−26054.

18. Zocchi, E., Franco, L., Guida, L., Benatti, U., Bargellesi, A., Malavasi, F., Lee, H. C., and De Flora, A. (1993) A single protein immunologically identified as CD38 displays NAD$^+$ glycohydrolase, ADP-ribosyl cyclase and cyclic ADP-ribosyl hydrolase activities at the outer surface of human erythrocytes, *Biochem. Biophys. Res. Commun. 196*, 1459−1465.

19. Summerhill, R. J., Jackson, D. G., and Galione, A. (1993) Human lymphocyte antigen CD38 catalyzes the production of cyclic ADP-ribose, *FEBS Lett. 335*, 231−233.

20. Hirata, Y., Kimura, N., Sato, K., Ohsugi, Y., Takasawa, S., Okamoto, H. I., Kaisho, T., Ishihara, K., and Hirano, T. (1994) ADP-ribosyl cyclase activity of a novel bone marrow stromal cell surface molecule BST-1, *FEBS Lett. 356*, 244−248.

21. Lee, H. C., and Aarhus, R. (1995) A derivative of NADP mobilizes calcium stores insensitive to inositol trisphosphate and cyclic ADP-ribose, *J. Biol. Chem. 270*, 2152−2157.

22. Aarhus, R., Graeff, R. M., Dickey, D. M., Walseth, T. F., and Lee, H. C. (1995) ADP-ribosyl cyclase and CD38 catalyze the synthesis of a calcium mobilizing metabolite from NADP, *J. Biol. Chem. 270*, 30327−30333.

23. Dargie, P. J., Agee, M. C., and Lee, H. C. (1990) Comparison of Ca2+ mobilizing activities of cyclic ADP-ribose and inositol triphosphate, *Cell Regul. 1*, 279−280.

24. Galione, A., Lee, H. C., and Busa, W. B. (1991) Ca^{2+}-induced Ca^{2+}release in sea urchin egg homogenates: modulation by cyclic ADP-ribose, *Science 253*, 1143−1146.

25. Lee, H. C. (1993) Potentiation of calcium- and caffeine-induced calcium release by cyclic ADP-ribose, *J. Biol. Chem. 268*, 293−299.

26. Meszaros, L., Bak, J., and Chu, A. (1993) Cyclic ADP-ribose as an endogenous regulator of the nonskeletal type ryanodine receptor Ca^{2+} channel, *Nature 354*, 76−78.

27. Mojzisova, A., Krizanova, O., Zacikova, L., Kominkova, V., and Ondrias, K. (2001) Effect of nicotinic acid adenine dinucleotide phosphate on ryanodine calcium release channel in heart, *Pflugers Arch. 441*, 674−677.

28. Hohenegger, M., Suko, J., Gscheidlinger, R., Drobny, H., and Zidar, A. (2002) Nicotinic acid-adenine dinucleotide phosphate activates the skeletal muscle ryanodine receptor, *Biochem. J. 367*, 423−431.

29. Gerasimenko, J. V., Maruyama, Y., Yano, K., Dolman, N. J., Tepikin, A. V., Petersen, O. H., and Gerasimenko, O. V. (2003) NAADP mobilizes Ca^{2+} from a thapsigargin-sensitive store in the nuclear envelope by activating ryanodine receptors, *J. Cell Biol. 163*, 271−282.

30. Langhorst, M. F., Schwarzmann, N., and Guse, A. H. (2004) Ca2+ release via ryanodine receptors and Ca^{2+} entry: major mechanisms in NAADP-mediated Ca^{2+} signaling in T-lymphocytes, *Cell. Signalling 16*, 1283−1289.

31. Dammermann, W., and Guse, A. H. (2005) Functional Ryanodine Receptor Expression Is Required for NAADP-mediated Local Ca^{2+} Signaling in T-lymphocytes, *J. Biol. Chem. 280*, 21394−21399.

32. Perraud, A. L., Fleig, A., Dunn, C. A., Bagley, L. A., Launay, P., Schmitz, C., Stokes, A. J., Zhu, Q., Bessman, M. J., Penner, R., Kinet, J. P., and Scharenberg, A. M. (2001) ADP-ribose gating of the calcium-permeable LTRPC2 channel revealed by Nudix motif homology, *Nature 411*, 595−599.

33. Hara, Y., Wakamori, M., Ishii, M., Maeno, E., Nishida, M., Yoshida, T., Yamada, H., Shimizu, S., Mori, E., Kudoh, J., Shimizu, N., Kurose, H., Okada, Y., Imoto, K., and Mori, Y. (2002) LTRPC2 Ca^{2+}-permeable channel activated by changes in redox status confers susceptibility to cell death, *Mol. Cell 9*, 163−173.

34. Sano, Y., Inamura, K., Miyake, A., Mochizuki, S., Yokoi, H., Matsushime, H., and Furuichi, K. (2001) Immunocyte Ca^{2+} influx system mediated by LTRPC2, *Science 293*, 1327−1330.

35. Galione, A. (2002) in *Cyclic ADP-ribose and NAADP. Structures, metabolism and functions* (Lee, H. C., Ed.) pp 45−64, Kluwer Academic Publishers, Dordrecht.

36. Cockayne, D., Muchamuel, T., Grimaldi, J. C., Muller-Steffner, H., Randall, T. D., Lund, F. E., Murray, R., Schuber, F., and Howard, M. C. (1998) Mice deficient for the ecto-NAD$^+$ glycohydrolase CD38 exhibit altered humoral immune responses, *Blood 92*, 1324−1333.

37. Kato, I., Yamamoto, Y., Fujimura, M., Noguchi, N., Takasawa, S., and Okamoto, H. (1999) CD38 disruption impairs glucose-induced increases in cyclic ADP-ribose, [Ca^{2+}]$_i$, and insulin secretion, *J. Biol. Chem. 274*, 1869−1872.

38. Partida-Sanchez, S., Goodrich, S., Kusser, K., Oppenheimer, N., Randall, T. D., and Lund, F. E. (2004) Regulation of dendritic cell trafficking by the ADP-ribosyl cyclase CD38: Impact on the development of humoral immunity, *Immunity 20*, 279−291.

39. Partida-Sanchez, S., Cockayne, D. A., Monard, S., Jacobson, E. L., Oppenheimer, N., Garvy, B., Kusser, K., Goodrich, S., Howard, M., Harmsen, A., Randall, T. D., and Lund, F. E. (2001) Cyclic ADP-ribose production by CD38 regulates intracellular calcium release, extracellular calcium influx and chemotaxis in neutrophils and is required for bacterial clearance *in vivo*, *Nat. Med. 7*, 1209−1216.

40. Deshpande, D. A., White, T. A., Guedes, A. G., Milla, C., Walseth, T. F., Lund, F. E., and Kannan, M. S. (2004) Altered airway responsiveness in CD38-deficient mice, *Am. J. Respir. Cell Mol. Biol. 32*, 149−156.

41. Thompson, M., Barata da Silva, H., Zielinska, W., White, T. A., Bailey, J. P., Lund, F. E., Sieck, G. C., and Chini, E. N. (2004) Role of CD38 in myometrial Ca^{2+} transients: modulation by progesterone, *Am. J. Physiol. Endocrinol. Metab. 287*, E1142−E1148.

42. Sun, L., Iqbal, J., Dolgilevich, S., Yuen, T., Wu, X. B., Moonga, B. S., Adebanjo, O. A., Bevis, P. J., Lund, F., Huang, C. L., Blair, H. C., Abe, E., and Zaidi, M. (2003) Disordered osteoclast

formation and function in a CD38 (ADP-ribosyl cyclase)-deficient mouse establishes an essential role for CD38 in bone resorption, *FASEB J. 17*, 369−375.

43. Fukushi, Y., Kato, I., Takasawa, S., Sasaki, T., Ong, B. H., Sato, M., Ohsaga, A., Sato, K., Shirato, K., Okamoto, H., and Maruyama, Y. (2001) Identification of cyclic ADP-ribose-dependent mechanisms in pancreatic muscarinic Ca^{2+} signaling using CD38 knockout mice, *J. Biol. Chem. 276*, 649−655.

44. Deshpande, D. A., Walseth, T. F., Panettieri, R. A., and Kannan, M. S. (2003) CD38/cyclic ADP-ribose-mediated Ca^{2+} signaling contributes to airway smooth muscle hyper-responsiveness, *FASEB J. 17*, 452−454.

45. Engels, D., Chitsulo, L., Montresor, A., and Savioli, L. (2002) The global epidemiological situation of schistosomiasis and new approaches to control and research, *Acta Trop. 82*, 139−146.

46. Freebern, W. J., Osman, A., Niles, E. G., Christen, L., and LoVerde, P. T. (1999) Identification of a cDNA encoding a retinoid X receptor homologue from Schistosoma mansoni. Evidence for a role in female-specific gene expression, *J. Biol. Chem. 274*, 4577−85.

47. Hu, W., Yan, Q., Shen, D. K., Liu, F., Zhu, Z. D., Song, H. D., Xu, X. R., Wang, Z. J., Rong, Y. P., Zeng, L. C., Wu, J., Zhang, X., Wang, J. J., Xu, X. N., Wang, S. Y., Fu, G., Zhang, X. L., Wang, Z. Q., Brindley, P. J., McManus, D. P., Xue, C. L., Feng, Z., Chen, Z., and Han, Z. G. (2003) Evolutionary and biomedical implications of a Schistosoma japonicum complementary DNA resource, *Nat. Genet. 35*, 139−147.

48. Higgins, D. G., Thompson, J. D., and Gibson, T. J. (1996) Using CLUSTAL for multiple sequence alignments, *Methods Enzymol. 266*, 383−402.

49. Marti-Renom, M. A., Stuart, A. C., Fiser, A., Sanchez, R., Melo, F., and Sali, A. (2000) Comparative protein structure modeling of genes and genomes, *Annu. Rev. Biophys. Biomol. Struct. 29*, 291−325.

50. Bendtsen, J. D., Nielsen, H., von Heijne, G., and Brunak, S. (2004) Improved prediction of signal peptides: SignalP 3.0, *J. Mol. Biol. 340*, 783−795.

51. Kall, L., Krogh, A., and Sonnhammer, E. L. (2004) A combined transmembrane topology and signal peptide prediction method, *J. Mol. Biol. 338*, 1027−1036.

52. Eisenhaber, B., Bork, P., and Eisenhaber, F. (1998) Sequence properties of GPI-anchored proteins near the omega-site: constraints for the polypeptide binding site of the putative transamidase, *Protein Eng. 11*, 1155−1161.

53. Woo, J. H., Liu, Y. Y., Mathias, A., Stavrou, S., Wang, Z., Thompson, J., and Neville, D. M., Jr. (2002) Gene optimization is necessary to express a bivalent anti-human anti-T cell immunotoxin in Pichia pastoris, *Protein Expression Purif. 25*, 270−282.

54. Clendenon, J. L., Phillips, C. L., Sandoval, R. M., Fang, S., and Dunn, K. W. (2002) Voxx: a PC-based, near real-time volume rendering system for biological microscopy, *Am. J. Physiol. 282*, C213−C218.

55. Muller, H. M., Muller, C. D., and Schuber, F. (1983) NAD+ glycohydrolase, an ecto-enzyme in calf spleen cells, *Biochem. J. 212*, 459−464.

56. Graeff, R. M., Walseth, T. F., Fryxell, K., Branton, W. D., and Lee, H. C. (1994) Enzymatic synthesis and characterization of cyclic GDP-ribose, *J. Biol. Chem. 269*, 30260−30267.

57. Graeff, R., and Lee, H. C. (2002) A novel cycling assay for cellular cADP-ribose with nanomolar sensitivity, *Biochem. J. 361*, 379−384.

58. Lund, F. E., Muller-Steffner, H. M., Yu, N., Stout, C. D., Schuber, F., and Howard, M. (1999) CD38 signaling is controlled by its ectodomain but occurs independently of enzymatically generated ADP-ribose or cyclic ADP-ribose, *J. Immunol. 162*, 2693−2702.

59. Osman, A., Niles, E. G., and LoVerde, P. T. (2004) Expression of functional Schistosoma mansoni Smad4: role in Erk-mediated transforming growth factor beta (TGF-beta) down-regulation, *J. Biol. Chem. 279*, 6474−6486.

60. Lee, H. C. (2004) Multiplicity of Ca^{2+} messengers and Ca^{2+} stores: a perspective from cyclic ADP-ribose and NAADP, *Curr. Mol. Med. 4*, 227−237.

61. Eisenhaber, B., Maurer-Stroh, S., Novatchkova, M., Schneider, G., and Eisenhaber, F. (2003) Enzymes and auxiliary factors for GPI lipid anchor biosynthesis and post-translational transfer to proteins, *BioEssays 25*, 367−385.

62. Cakir-Kiefer, C., Muller-Steffner, H., Oppenheimer, N., and Schuber, F. (2001) Kinetic competence of the cADP-ribose-CD38 complex as an intermediate in the CD38/NAD^+ glycohydrolase-catalysed reactions: implication for CD38 signalling, *Biochem. J. 358*, 399−406.

63. Berthelier, V., Tixier, J.-M., Muller-Steffner, H., Schuber, F., and Deterre, P. (1998) Human CD38 is an authentic $NAD(P)^+$ glycohydrolase, *Biochem. J. 330*, 1383−1390.

64. Zatman, L. J., Kaplan, N. O., Colowick, S. P., and Ciotti, M. M. (1954) Effect of isonicotinic acid hydrazide on diphosphopyridine nucleotidases, *J. Biol. Chem. 209*, 453−466.

65. Muller-Steffner, H., Muzard, M., Oppenheimer, N., and Schuber, F. (1994) Mechanistic implications of cyclic ADP-Ribose hydrolysis and methanolysis catalyzed by calf spleen NAD^+-Glycohydrolase, *Biochem. Biophys. Res. Commun. 204*, 1279−1285.

66. Erasmus, D. A. (1987) in *The Biology of Schistosomes, from Genes to Latrines*, pp 51−82, Academic Press, New York.

67. Muller, C. D., Tarnus, C., and Schuber, F. (1984) Preparation of analogues of NAD^+ as substrates for a sensitive fluorimetric assay of nucleotide pyrophosphatase, *Biochem. J. 223*, 715−721.

68. Ferrero, E., and Malavasi, F. (2002) in *Cyclic ADP-ribose and NAADP: Structures, metabolism and functions* (Lee, H. C., Ed.) pp 65−80, Kluwer Academic Publishers, Dordrecht.

69. Kim, H., Jacobson, E. L., and Jacobson, M. K. (1993) Synthesis and degradation of cyclic ADP-ribose by NAD glycohydrolases, *Science 261*, 1330−1333.

70. Muller-Steffner, H. M., Augustin, A., and Schuber, F. (1996) Mechanism of cyclization of pyridine nucleotides by bovine spleen NAD+ glycohydrolase, *J. Biol. Chem. 271*, 23967−23972.

71. Sauve, A. A., Munshi, C., Lee, H. C., and Schramm, V. L. (1998) The reaction mechanism for CD38. A single intermediate is responsible for cyclization, hydrolysis, and base-exchange chemistries, *Biochemistry 37*, 13239−13249.

72. Wolde Mussie, E., Vande Waa, J., Pax, R. A., Fetterer, R., and Bennett, J. L. (1982) Schistosoma mansoni: calcium efflux and effects of calcium-free media on responses of the adult male musculature to praziquantel and other agents inducing contraction, *Exp. Parasitol. 53*, 270−278.

73. Redman, C. A., Robertson, A., Fallon, P. G., Modha, J., Kusel, J. R., Doenhoff, M. J., and Martin, R. J. (1996) Praziquantel: An urgent and exciting challenge, *Parasitol. Today 12*, 14−20.

74. Kohn, A. B., Anderson, P. A., Roberts-Misterly, J. M., and Greenberg, R. M. (2001) Schistosome calcium channel beta subunits. Unusual modulatory effects and potential role in the action of the antischistosomal drug praziquantel, *J. Biol. Chem. 276*, 36873−36876.

75. Silva, C. L., Cunha, V. M., Mendonca-Silva, D. L., and Noel, F. (1998) Evidence for ryanodine receptors in Schistosoma mansoni, *Biochem. Pharmacol. 56*, 997−1003.

76. Silva, C. L., Mendonca-Silva, D. L., and Noel, F. (1998) Evidence for functional ryanodine receptors in Schistosoma mansoni and their putative role in the control of calcium homeostasis, *Mem. Inst. Oswaldo Cruz 93* (Suppl. 1), 269−270.

77. Day, T. A., Haithcock, J., Kimber, M., and Maule, A. G. (2000) Functional ryanodine receptor channels in flatworm muscle fibres, *Parasitology 120* (Part 4), 417−422.

78. Day, T. A., Orr, N., Bennett, J. L., and Pax, R. A. (1993) Voltage-gated currents in muscle cells of Schistosoma mansoni, *Parasitology 106* (Part 5), 471−477.

79. Seman, M., Adriouch, S., Haag, F., and Koch-Nolte, F. (2004) Ecto-ADP-ribosyltransferases (ARTs): emerging actors in cell communication and signaling, *Curr. Med. Chem. 11*, 857−872.

80. Seman, M., Adriouch, S., Scheuplein, F., Krebs, C., Freese, D., Glowacki, G., Deterre, P., Haag, F., and Koch-Nolte, F. (2003) NAD-induced T cell death: ADP-ribosylation of cell surface proteins by ART2 activates the cytolytic P2X7 purinoceptor, *Immunity 19*, 571−582.

81. Itoh, M., Ishihara, K., Hiroi, T., Lee, B. O., Maeda, H., Iijima, H., Yanagita, M., Kiyono, H., and Hirano, T. (1998) Deletion of bone marrow stromal cell antigen-1 (CD157) gene impaired systemic thymus independent-2 antigen-induced IgG3 and mucosal TD antigen-elicited IgA responses, *J. Immunol. 161*, 3974−3983.

82. LoVerde, P. T. (1998) Do antioxidants play a role in schistosome host-parasite interactions?, *Parasitol. Today 14*, 284−289.

83. Muller-Steffner, H., Malver, O., Oppenheimer, N. J., and Schuber, F. (1992) Slow-binding inhibition of NAD^+ glycohydrolase by arabino analogues of β-NAD^+, *J. Biol. Chem. 267*, 9606−9611.